

Chapter One

1.1 Introduction

Lower limb peripheral arterial disease is a marker for increased risk of cardiovascular events even when it is asymptomatic. The most common initial symptom of peripheral arterial disease is leg pain while walking, known as intermittent claudication. Critical limb ischemia is a severe manifestation of peripheral arterial disease, and is characterized by severely diminished circulation, ischaemic pain, ulceration, tissue loss and/or gangrene. The incidence of peripheral arterial disease increases with age. Population studies have found that about 20% of people aged over 60 years have some degree of peripheral arterial disease. Incidence is also high in people who smoke, people with diabetes and people with coronary artery disease. In most people with intermittent claudication the symptoms remain stable, but approximately 20% will develop increasingly severe symptoms with the development of critical limb ischemia. Rapid changes in diagnostic methods, endovascular treatments and vascular services, associated with the emergence of new sub-specialties in surgery and interventional radiology, has resulted in considerable uncertainty and variation in practice. This guideline aims to resolve that uncertainty and variation. The majority of deaths in western societies such as the United States are attributed in large part to arteriosclerosis, or hardening and thickening of the arterial wall. Underlying peripheral vascular disease as well as coronary artery and cerebrovascular disease is atherosclerosis, a disorder of larger arteries and one type of arteriosclerosis. Atherosclerosis is the leading cause of death in the general population in industrialized countries. It is well recognized that hypertension plays a major role in the pathogenesis of atherosclerotic vascular disease. This has important implications from a public health perspective because of the high prevalence of hypertension and its amenability to effective treatment (Criqui et al 1985).

The mechanism for the pathogenesis of atherosclerosis is generally considered separate from hypertension. Hypertension, however, accelerates the atherosclerotic process in large part as a result of increased shear stress on arterial walls. This increased shear stress stimulates a variety of proliferative growth factors, e.g., platelet-derived growth factor, endothelin, and others that ultimately enhance the atherosclerotic process. This process is exemplified by the Charcot-Bouchard aneurysms and fibrinoid arteriolar necrosis seen in hypertensives (Murphy, et al 2000). This chapter will focus on the epidemiology of peripheral vascular disease seen among hypertensive subjects. It will delineate both the incidence and prevalence of this disease, as well as elucidate risk factors for the development of peripheral vascular disease in hypertensive populations.

Coronary arterial disease, carotid artery disease, and Lower Extremity Arterial Disease (LEAD) have many causes. Risk factors associated with these disease entities, which can be modified are: cigaret smoking, arterial hypertension, diabetes mellitus, various dislipidemias, i.e., hypertriglyceridemia in particular for LEAD, high low-density lipoprotein (LDL) cholesterol particularly for coronary artery disease, high lipoprotein(a) [Lp(a)], low high-density lipoprotein (HDL) cholesterol, obesity, homocysteinemia, elevated high sensitivity C-reactive protein (CRP), and physical inactivity. Significant progress has been made to lower the trend for cigaret smoking in the United States and other industrialized countries through educational programs for the public, reviews by the press, legislative action at all three levels of government (local, state, and federal), as well as landmark decisions by the judiciary (Murphy, et al 2000).

The pioneering work of the American Heart Association in initiating smoking cessation programs was closely followed by the American Lung Association, the American Cancer Society, the World Health Organization, and more recently by the European Union.

Not much progress has been made with regards to obesity and physical inactivity as risk factors for cardiovascular disease (CVD). Since 1970, obesity in the United States has become a public health problem and continues to grow. The concept that sedentary lifestyle may lead to an increase in prevalence of CVD, especially myocardial infarction (MI) and sudden cardiac death, has been recognized by cardiovascular physicians and all health care providers (Murphy, et al 2000).

Data relating to the level of regular exercise and risk for all CVDs have been derived from a variety of sources, including annual patient studies, observational studies, prospective studies, and retrospective studies (McDermott et al 2000)

No study has been executed so far that provides biological evidence of the cause or causes, biochemical link or links, between exercise status and cardiovascular morbidity and mortality or the specific pathophysiology of physical inactivity. The basic biological progression of atherosclerosis at the molecular level continues to be studied and is gradually being established (13). The existing observational studies can only provide inferences and associations between the predictive value for the development of coronary artery disease, LEAD, and physical inactivity (12).

For the past 50 years, more than 50 published studies have reported the protective effect of regular exercise on the development and deceleration of progression of CVD. Physically active cardiovascular patients.

Atherosclerotic disease is diffuse in nature. As cardiologists, we tend to focus upon atherosclerosis of the coronary arteries and the resultant complications; however, atherosclerosis of the peripheral arterial system contributes to significant morbidity and mortality in our patients. As the role of the Cardiologist becomes increasingly broader and encompasses cardiovascular diseases in general, it is imperative that we learn the significance of lower extremity peripheral arterial Disease (PAD).

This review will discuss the importance of PAD. Anatomic and physiologic definitions of lower extremity atherosclerotic occlusive arterial disease as well as its pathophysiology will be discussed. The prevalence of PAD in various populations as well as risk factors for the development of atherosclerotic disease will be presented. The natural history, including morbidity and mortality concerns of PAD, will be reviewed (McDermott et al 2000).

Treatment options will be reviewed only in brief. The intent of this review is to develop a greater appreciation for PAD and update cardiovascular medicine specialists on this disease.

Some readers may ask, “if PAD is generally from atherosclerosis and most of our patients have coronary artery disease (CAD), what is the rationale of looking for PAD if our recommendations will not be changed?” By being educated in lower extremity PAD, the clinician will be able to increase the quality of life of the patient and substantially reduce the associated morbidity and mortality of this disease. The role of the cardiologist is expanding into that of a cardiovascular medicine specialist due to many advances in preventive, medical, rehabilitative, and interventional therapies.

1.2 Problem of study:

Multi-Detector Row Computed Tomography Angiography (MDCTA) is increasingly used to peripheral arterial disorders to diagnosis any abnormalities of artery and venous, and There is no reference for Sudanese patient for measurement of abdominal aorta and common femoral artery in CT Angiography for normal patients.

therefore, evaluation of lower limb disease can be accomplished in a short period of time and ability to create 3D image for useful diagnosis, the lower limb disease can be done more accurately than other modalities like U/S and MRI, exploration of this capabilities will be of a great value for the diagnosis and management.

1.3 Justification

With the introduction of multi-detector row computed tomography (MDCT), scan speed and image quality has improved considerably. Since the longitudinal coverage is no longer a limitation, multi-detector row computed tomography angiography (MDCTA) is increasingly used to depict the peripheral arterial runoff. Hence, it is important to know the advantages and limitations of this new non-invasive alternative for the reference test, digital subtraction angiography. Optimization of the acquisition parameters and the contrast delivery is important to achieve a reliable enhancement of the entire arterial runoff in patients with peripheral arterial disease (PAD) using fast CT scanners.

1.4 Objectives of the study:

The general objective of this study is to characterize lower limb disease using MDCT in order to evaluate the diameter of abdominal aorta at its bifurcation to left and right common femoral artery.

1.5 Specific objective

- To find the cross-correlate for common femoral artery parts (Lt, Rt and Upper) with gender.
- To measure the ratio of the arterial stenosis of the lower arterial limb diseases
- To measure the dimensions of the lower limb for diabetic and hypertensive patients.
- To correlate the lower limb disease for diabetic and hypertensive patient
- To find the sensitivity, specificity and accuracy of MDCT in diagnosing arterial lower limb disease
- To characterize of abdominal aorta at its bifurcation to left and right common femoral artery.
- To find the difference between the left and right common femoral artery side.
- To measure the ratio of the arterial stenosis of the lower arterial limb diseases

- To correlate between the normal and diabetic patients in common femoral artery diameter and the abdominal aorta bifurcation.

1.6 Overview of the study

This study falls into five chapters. Chapter one is consist of introduction, problem of the study, general, specific objectives and significant of the study. Chapter two concerns with literature review. Chapter three is about the methodology which includes material and method, chapter four about the result presentation, chapter five about the discussion, conclusion, recommendation and limitations including the references and appendixes.

Chapter Two

2.1 Anatomy:

2.1.1 Introduction:

Lower Limb Disorders (LLDs) at work affect the hips, knees and legs and usually happen because of overuse - workers may report lower limb pain, aching and numbness without a specific disease being identified, Acute injury caused by a violent impact or extreme force is less common. However, athletes and military personnel are more prone to these injuries so workers who take part in these activities may report them at work (Henry Gray et al 2001).

Scientific evidence suggests that there are several recognized diseases of the lower limb which can be work related such as: hip and knee osteoarthritis; knee bursitis, meniscal lesions/tears; stress fracture/reaction injury and varicose veins of the lower legs.

Lower limb artery disease also referred to as peripheral artery disease (PAD) is the most common disease which occurs when the blood vessels that supply blood to the limbs and other organs of our body are partially or completely blocked due to plaque build-up. This is a condition called atherosclerosis. Plaque forms out of the substances present in blood such as fat, cholesterol, calcium and fibrous tissue. These plaque deposits gradually harden and narrow the opening of the arteries. This limits the oxygen-rich blood supply to the parts of your body. The most commonly affected blood vessels due to PVD are the arteries of the legs(Henry Gray et al 2001).

2.1.2 Causes and Risk Factors

The most common cause of lower limb artery disease is atherosclerosis. Other causes include:

Formation of blood clot (thrombus/emboli) that may block a blood vessel. high blood sugar levels with associated high cholesterol may damage the blood vessels over a long term. Inflammation of

the arteries (arteritis) can weaken and narrow down the arteries, Infections such as salmonellosis and syphilis can infect and damage the blood vessels.

Several factors are considered to increase the risk of developing lower limb artery disease and they include family history of heart attacks or strokes, increased age (>50 years), overweight, sedentary lifestyle, smoking, diabetes, hypertension, dyslipidaemia, and past history of coronary heart disease, heart attack, or stroke.

2.1.3 Mechanism of the Pelvis:

The pelvic girdle supports and protects the contained viscera and affords surfaces for the attachments of the trunk and lower limb muscles. Its most important mechanical function, however, is to transmit the weight of the trunk and upper limbs to the lower extremities. It may be divided into two arches by a vertical plane passing through the acetabular cavities; the posterior of these arches is the one chiefly concerned in the function of transmitting the weight. Its essential parts are the upper three sacral vertebrae and two strong pillars of bone running from the sacroiliac articulations to the acetabular cavities. For the reception and diffusion of the weight each acetabular cavity is strengthened by two additional bars running toward the pubis and ischium. In order to lessen concussion in rapid changes of distribution of the weight, joints (sacroiliac articulations) are interposed between the sacrum and the iliac bones; an accessory joint (pubic symphysis) exists in the middle of the anterior arch. The sacrum forms the summit of the posterior arch; the weight transmitted falls on it at the lumbosacral articulation and, theoretically, has a component in each of two directions. One component of the force is expended in driving the sacrum downward and backward between the iliac bones, while the other thrusts the upper end of the sacrum downward and forward toward the pelvic cavity (Henry Gray et al 2001).

The movements of the sacrum are regulated by its form. Viewed as a whole, it presents the shape of a wedge with its base upward and forward. The first component of the force is therefore acting against the resistance of the wedge, and its tendency to separate the iliac bones is resisted by the sacroiliac and iliolumbar ligaments and by the ligaments of the pubic symphysis(Henry Gray et al 2001).

2.1.4 The Ligamentum Teres Femoris:

The ligamentum teres femoris is a triangular, somewhat flattened band implanted by its apex into the antero-superior part of the fovea capitis femoris; its base is attached by two bands, one into either side of the acetabular notch, and between these bony attachments it blends with the transverse ligament. It is ensheathed by the synovial membrane, and varies greatly in strength in different subjects; occasionally only the synovial fold exists, and in rare cases even this is absent. The ligament is made tense when the thigh is semiflexed and the limb then adducted or rotated outward; it is, on the other hand, relaxed when the limb is abducted. It has, however, but little influence as a ligament(Henry Gray et al 2001).

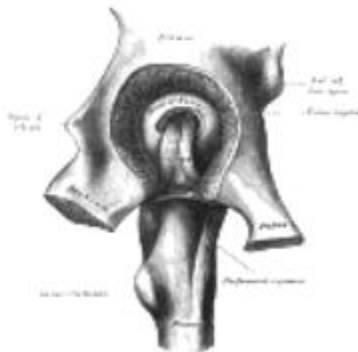


FIG 2.1. Capsule of right knee-joint (distended). Posterior aspect

2.1.5 Movements:

The movements which take place at the knee-joint are flexion and extension, and, in certain positions of the joint, internal and external rotation. The movements of flexion and extension at this joint differ from those in a typical hinge-joint, such as the elbow, in that (*a*) the axis around which motion takes place is not a fixed one, but shifts forward during extension and backward during flexion; (*b*) the commencement of flexion and the end of extension are accompanied by rotatory movements associated with the fixation of the limb in a position of great stability. The movement from full flexion to full extension may therefore be described in three phases:

1. In the fully flexed condition the posterior parts of the common femoral condyles rest on the corresponding portions of the meniscotibial surfaces, and in this position a slight amount of simple rolling movement is allowed.
2. During the passage of the limb from the flexed to the extended position a gliding movement is superposed on the rolling, so that the axis, which at the commencement is represented by a line through the inner and outer condyles of the femur, gradually shifts forward. In this part of the movement, the posterior two-thirds of the tibial articular surfaces of the two common femoral condyles are involved, and as these have similar curvatures and are parallel to one another, they move forward equally.
3. The lateral condyle of the femur is brought almost to rest by the tightening of the anterior cruciate ligament; it moves, however, slightly forward and medialward, pushing before it the anterior part of the lateral meniscus. The tibial surface on the medial condyle is prolonged farther forward than that on the lateral, and this prolongation is directed lateralward. When, therefore, the movement forward of the condyles is checked by the anterior cruciate ligament, continued

muscular action causes the medial condyle, dragging with it the meniscus, to travel backward and medialward, thus producing an internal rotation of the thigh on the leg(Henry Gray et al 2001).

When the position of full extension is reached the lateral part of the groove on the lateral condyle is pressed against the anterior part of the corresponding meniscus, while the medial part of the groove rests on the articular margin in front of the lateral process of the tibial intercondyloid eminence. Into the groove on the medial condyle is fitted the anterior part of the medial meniscus, while the anterior cruciate ligament and the articular margin in front of the medial process of the tibial intercondyloid eminence are received into the forepart of the intercondyloid fossa of the femur. This third phase by which all these parts are brought into accurate apposition is known as the “screwing home,” or locking movement of the joint(Henry Gray et al 2001).

The complete movement of flexion is the converse of that described above, and is therefore preceded by an external rotation of the femur which unlocks the extended joint. The axes around which the movements of flexion and extension take place are not precisely at right angles to either bone; in flexion, the femur and tibia are in the same plane, but in extension the one bone forms an angle, opening lateralward with the other. In addition to the rotatory movements associated with the completion of extension and the initiation of flexion, rotation inward or outward can be effected when the joint is partially flexed; these movements take place mainly between the tibia and the menisci, and are freest when the leg is bent at right angles with the thigh(Henry Gray et al 2001).

Movements of Patella.—The articular surface of the patella is indistinctly divided into seven facets—upper, middle, and lower horizontal pairs, and a medial perpendicular facet.

When the knee is forcibly flexed, the medial perpendicular facet is in contact with the semilunar surface on the lateral part of the medial condyle; this semilunar surface is a prolongation backward of the medial part of the patellar surface.

As the leg is carried from the flexed to the extended position, first the highest pair, then the middle pair, and lastly the lowest pair of horizontal facets is successively brought into contact with the patellar surface of the femur. In the extended position, when the Quadriceps femoris is relaxed, the patella lies loosely on the front of the lower end of the femur(Henry Gray et al 2001).

During flexion, the ligamentum patellæ is put upon the stretch, and in extreme flexion the posterior cruciate ligament, the oblique popliteal, and collateral ligaments, and, to a slight extent, the anterior cruciate ligament, are relaxed. Flexion is checked during life by the contact of the leg with the thigh. When the knee-joint is fully extended the oblique popliteal and collateral ligaments, the anterior cruciate ligament, and the posterior cruciate ligament, are rendered tense; in the act of extending the knee, the ligamentum patellæ is tightened by the Quadriceps femoris, but in full extension with the heel supported it is relaxed. Rotation inward is checked by the anterior cruciate ligament; rotation outward tends to uncross and relax the cruciate ligaments, but is checked by the tibial collateral ligament. The main function of the cruciate ligament is to act as a direct bond between the tibia and femur and to prevent the former bone from being carried too far backward or forward. They also assist the collateral ligaments in resisting any bending of the joint to either side. The menisci are intended, as it seems, to adapt the surfaces of the tibia to the shape of the common femoral condyles to a certain extent, so as to fill up the intervals which would otherwise be left in the varying positions of the joint, and to obviate the jars which would be so frequently transmitted up the limb in jumping or by falls on the feet; also to permit of the two varieties of motion, flexion and extension, and rotation, as explained above. The patella is a great defence to the front of the knee-joint, and distributes upon a large and tolerably even surface, during kneeling, the pressure which would otherwise fall upon the prominent ridges of the condyles; it also affords leverage to the Quadriceps femoris(Henry Gray et al 2001).



FIG2.2. Posterior surface of the right patella, showing diagrammatically the areas of contact with the femur in different positions of the knee

When standing erect in the attitude of “attention,” the weight of the body falls in front of a line carried across the centers of the knee-joints, and therefore tends to produce overextension of the articulations; this, however, is prevented by the tension of the anterior cruciate, oblique popliteal, and collateral ligaments.

Extension of the leg on the thigh is performed by the Quadriceps femora's; *flexion* by the Biceps femora's, Semitendinosus, and Semimembranosus, assisted by the Gracilize, Sartorius, Gastrocnemius, Popliteus, and Plantar is. *Rotation outward* is effected by the Biceps femora's, and *rotation inward* by the Popliteus, Semitendinosus, and, to a slight extent, the Semimembranosus, the Sartorius, and the Gracilize. The Popliteus comes into action especially at the commencement of the movement of flexion of the knee; by its contraction the leg is rotated inward, or, if the tibia be fixed, the thigh is rotated outward, and the knee-joint is unlocked (Henry Gray et al 2001).

2.1.6 Branches of the Abdominal Portion of the Aorta:

The abdominal portion of the aorta is the segment of the aorta between the diaphragm and the level of the fourth lumbar vertebra, where it divides into the right and left common iliac arteries.

Small inferior phrenic arteries that serve the diaphragm are the first vessels to arise from the abdominal portion of the aorta. The next vessel is the short and thick celiac (*se'le-ak*) trunk, an unpaired vessel that divides immediately into three arteries: the splenic, going to the spleen; the left gastric, going to the stomach; and the common hepatic, going to the liver (figs. 16.28 and 16.29). The superior mesenteric artery is another unpaired vessel. It arises anteriorly from the abdominal portion of the aorta, just below the celiac trunk. The superior mesenteric artery supplies blood to the small intestine (except for a portion of the duodenum), the cecum, the appendix, the ascending colon, and the proximal two-thirds of the transverse colon.

The next major vessels to arise from the abdominal portion of the aorta are the paired renal arteries that carry blood to the kidneys. Smaller suprarenal arteries, located just above the renal arteries, serve the adrenal (suprarenal) glands. The testicular arteries in the male and the ovarian arteries in the female are small paired vessels that arise from the abdominal portion of the aorta, just below the renal arteries. These vessels serve the gonads. The inferior mesenteric artery is the last major branch of the abdominal portion of the aorta. It is an unpaired anterior vessel that arises just before the iliac bifurcation. The inferior mesenteric supplies blood to the distal one-third of the transverse colon, the descending colon, the sigmoid colon, and the rectum.

Several lumbar arteries branch posteriorly from the abdominal portion of the aorta throughout its length and serve the muscles and the spinal cord in the lumbar region. In addition, an unpaired middle sacral artery arises from the posterior terminal portion of the abdominal portion of the aorta to supply the sacrum and coccyx.

2.1.7 Arteries of the Pelvis and Lower Extremity

The abdominal portion of the aorta terminates in the posterior pelvic area as it bifurcates into the right and left common iliac arteries. These vessels pass downward approximately 5 cm on their respective sides and terminate by dividing into the *internal* and *external iliac arteries*.

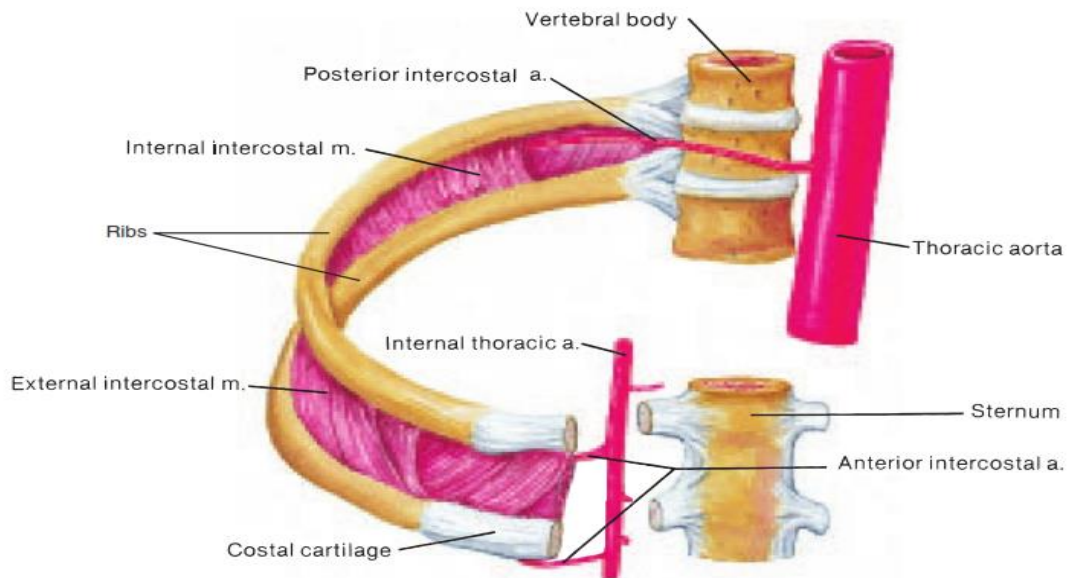
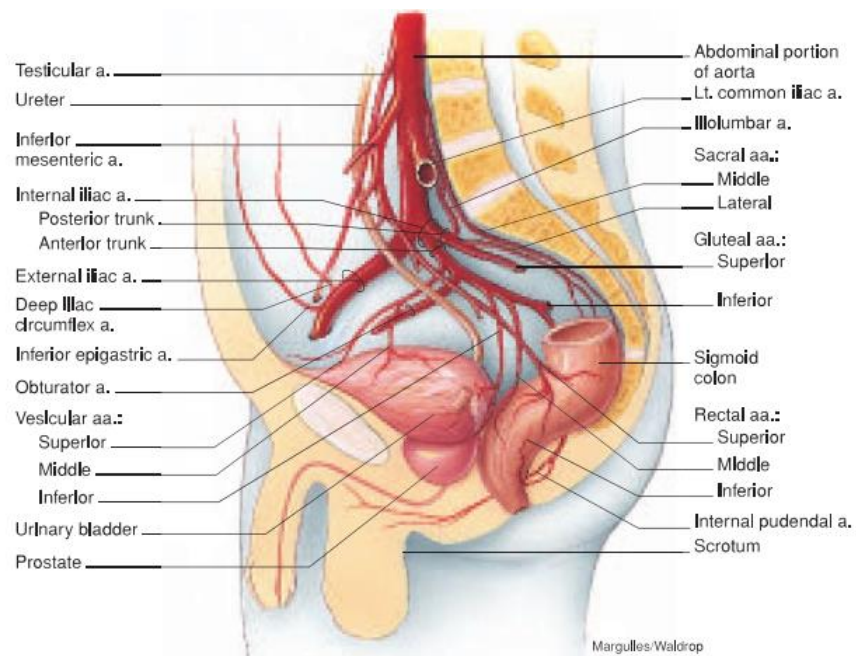


Fig 2.3 The *internal iliac artery* has extensive branches to supply arterial blood to the gluteal muscles and the organs of the pelvic region. The wall of the pelvis is served by the iliolumbar and lateral sacral arteries. The internal visceral organs of the pelvis are served by the middle rectal and the superior, middle, and inferior vesicular arteries to the urinary bladder. In addition, uterine and vaginal arteries branch from the internal iliac arteries to serve the reproductive organs of the female. The muscles of the buttock are served by the superior and inferior gluteal arteries. Some of the upper medial thigh muscles are supplied with blood from the obturator artery. The internal pudendal artery of the internal iliac artery serves the musculature of the perineum and the external genitalia. During sexual arousal it supplies the blood for vascular engorgement of the penis in the male and clitoris in the female.

The external iliac artery passes out of the pelvic cavity deep to the inguinal ligament (fig. 16.31) and becomes the common femoral (*fem'or-al*) artery. Two branches arise from the external iliac artery, however, before it passes beneath the inguinal ligament.

An inferior epigastric artery branches from the external iliac artery and passes superiorly to supply the skin and muscles of the abdominal wall. The deep circumflex iliac artery is a small branch that extends laterally to supply the muscles attached to the iliac fossa.

The common femoral artery passes through an area called the common femoral triangle on the upper medial portion of the thigh. At this point, it is close to the surface and its pulse can be palpated. Several vessels arise from the common femoral artery to serve the thigh region. The largest of these, the deep common femoral artery, passes posteriorly to serve the ham string muscles. The lateral and medial common femoral circumflex arteries encircle the proximal end of the femur and serve muscles in this region. The common femoral artery becomes the popliteal (*pop"li~te'al*) artery as it passes across the posterior aspect of the knee.



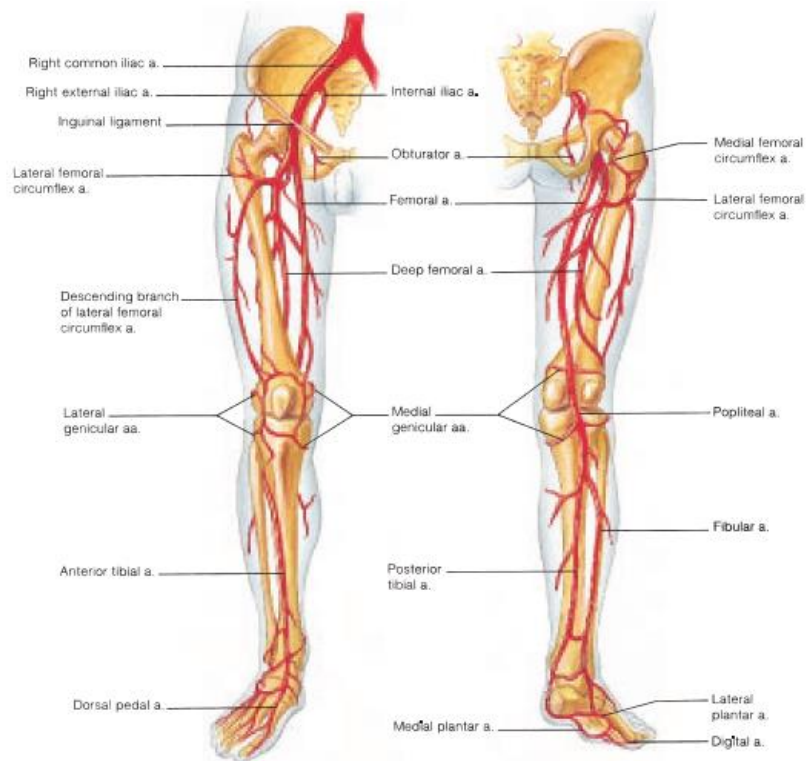


(Fig. 2.4) The popliteal artery supplies small branches to the knee joint, and then divides into an anterior tibial artery and a posterior tibial artery. These vessels traverse the anterior and posterior aspects of the leg, respectively, providing blood to the muscles of these regions and to the foot. At the ankle, the anterior tibial artery becomes the dorsal pedal artery that serves the ankle and dorsum (superior portion) of the foot and then contributes to the formation of the dorsal arch of the foot. Clinically, palpation of the dorsal pedal artery can provide information about circulation to the foot; more important, it can provide information about the circulation in general because its pulse is taken at the most distal portion of the body. The posterior tibial artery gives off a large fibular, or peroneal, artery to serve the peroneal muscles of the leg. At the ankle, the posterior tibial bifurcates into the lateral and medial plantar arteries that supply the sole of the foot.

2.2 Physiology:

2.2.1 Effect of High Right Atrial Pressure on Peripheral Venous Pressure:

When the right atrial pressure rises above its normal value of 0 mm Hg, blood begins to back up in the large veins. This backup of blood enlarges the veins, and even the collapse points in the veins open up when the right atrial pressure rises above 4 to 6 mm Hg(John E. Hall et al 2006).

Effect of Intra-abdominal Pressure on Venous Pressures of the Leg: The pressure in the abdominal cavity of a recumbent person normally averages about 6 mm Hg.

Effect of Gravitational Pressure on Venous Pressure: In any body of water that is exposed to air, the pressure at the surface of the water is equal to atmospheric pressure, but the pressure rises 1 mm Hg for each 13.6 millimeters of distance below the surface. This pressure results from the weight of the water and therefore is called gravitational pressure or hydrostatic pressure.

Gravitational pressure also occurs in the vascular system of the human being because of weight of the blood in the vessels. When a person is standing, the pressure in the right atrium remains about 0 mm Hg. In the arm veins, the pressure at the level of the top rib is usually about 6 mm Hg. In the leg veins, the pressure at the level of the top rib is usually about 6 mm Hg. (John E. Hall et al 2006).

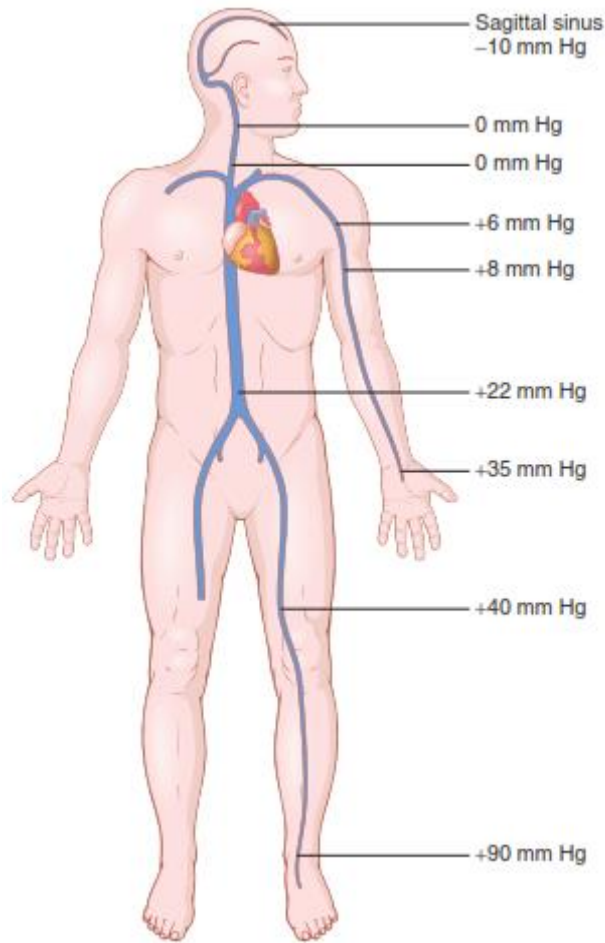


Fig 2.5 effect of gravitational pressure on the venous pressures throughout the body in the standing person

of the subclavian vein as it passes over this rib. The gravitational pressure down the length of the arm then is determined by the distance below the level of this rib. Thus, if the gravitational difference between the level of the rib and the hand is 29 mm Hg compression of the vein as it crosses the rib, making a total of 35 mm Hg almost completely all the way to the skull because of atmospheric pressure on the outside of the neck. This collapse causes the pressure in these veins to remain at zero along their entire extent. Any tendency for the pressure to rise above this level opens the veins and allows the pressure to fall back to zero because of flow of the blood.

Conversely, any tendency for the neck vein pressure to fall below zero collapses the veins still more, which further increases their resistance and again returns the pressure back to zero. The veins inside the skull, on the other hand, are in a noncollapsible chamber (the skull cavity) and thus they cannot collapse.

2.2.2 Effect of the Gravitational Factor on Arterial and Other Pressures:

The gravitational factor also affects pressures in the peripheral arteries and capillaries. For instance, a standing person who has a mean arterial pressure of 100 mm Hg at the level of the heart has an arterial pressure in the feet of about 190 mm Hg. Therefore, when one states that the arterial pressure is 100 mm Hg, this statement generally means that 100 mm Hg is the pressure at the gravitational level of the heart but not necessarily elsewhere in the arterial vessels (John E. Hall et al 2006).

2.2.3 Venous Valves and the “Venous Pump”:

Their Effects on Venous Pressure Were it not for valves in the veins, the gravitational pressure effect would cause the venous pressure in the feet always to be about 190 mm Hg in a standing adult. However, every time one moves the legs, one tightens the muscles and compresses the veins in or adjacent to the muscles, which squeezes the blood out of the veins.

However, they are arranged so that the direction of venous blood flow can be only toward the heart. Consequently, every time a person moves the legs or even tenses the leg muscles, a certain amount of venous blood is propelled toward the heart. This pumping system is known as the “venous pump” or “muscle pump,” and it is efficient enough that under ordinary circumstances the venous pressure in the feet of a walking adult remains less than 20 mm Hg (John E. Hall et al 2006).

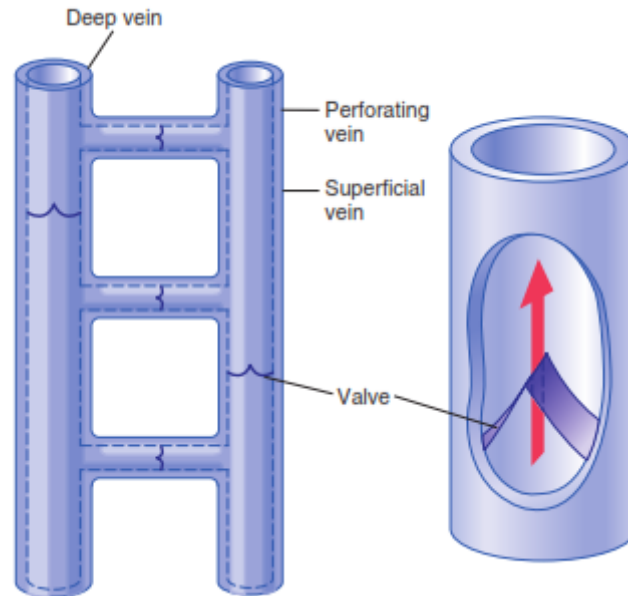


Fig 2.6 venous valves of the leg

If a person stands perfectly still, the venous pump does not work, and the venous pressures in the lower legs increase to the full gravitational value of 90 mm Hg in about 30 seconds. The pressures in the capillaries also increase greatly, causing fluid to leak from the circulatory system into the tissue spaces. As a result, the legs swell and the blood volume diminishes. Indeed, 10 to 20 percent of the blood volume can be lost from the circulatory system within the 15 to 30 minutes of standing absolutely still, which may lead to fainting as sometimes occurs when a soldier is made to stand at rigid attention. This situation can be avoided by simply flexing the leg muscles periodically and slightly bending the knees, thus permitting the venous pump to work(John E. Hall et al 2006).

2.2.4 Venous Valve Incompetence Causes “Varicose”Veins:

The valves of the venous system may become “incompetent” or even be destroyed when the veins have been overstretched by excess venous pressure lasting weeks or months, which can occur in pregnancy or when one stands most of the time. Stretching the veins increases their cross-sectional areas, but the leaflets of the valves do not increase in size. Therefore, the leaflets of the valves no longer close completely. When this lack of complete closure occurs, the pressure in the veins of the legs increases greatly because of failure of the venous pump, which further increases the sizes of the veins and finally destroys the function of the valves entirely. Thus, the person develops “varicose veins,” which are characterized by large, bulbous protrusions of the veins beneath the skin of the entire leg, particularly the lower leg(John E. Hall et al 2006).

Whenever people with varicose veins stand for more than a few minutes, the venous and capillary pressures become very high and leakage of fluid from the capillaries causes constant edema in the legs. The edema in turn prevents adequate diffusion of nutritional materials from the capillaries to the muscle and skin cells, so the muscles become painful and weak and the skin may even become gangrenous and ulcerate. The best treatment for such a condition is continual elevation of the legs to a level at least as high as the heart. Tight binders or long “compression” stockings on the legs also can be of considerable assistance in preventing the edema and its sequelae.

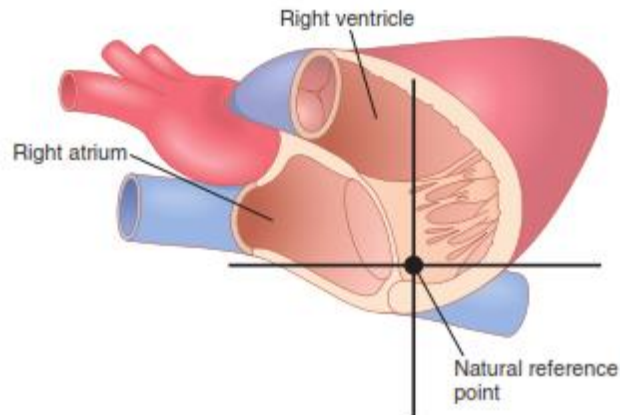


Figure 2.7 reference for circulatory pressure measurement (located near the tricuspid valve)

with ease by inserting a needle directly into a vein and connecting it to a pressure recorder. The only means by which right atrial pressure can be measured accurately is by inserting a catheter through the peripheral veins and into the right atrium. Pressures measured through such central venous catheters are often used in some types of hospitalized cardiac patients to provide constant assessment of heart-pumping ability(John E. Hall et al 2006).

2.2.5 Blood Reservoir Function of the Veins:

As pointed out in Chapter 14, more than 60 percent of all the blood in the circulatory system is usually in the veins. For this reason, and also because the veins are so compliant, it is said that the venous system serves as a blood reservoir for the circulation.

When blood is lost from the body and the arterial pressure begins to fall, nervous signals are elicited from the carotid sinuses and other pressure-sensitive areas of the circulation, as discussed in Chapter 18. These signals, in turn, elicit nerve signals from the brain and spinal cord, mainly through sympathetic nerves to the veins, causing them to constrict. This process takes up much of the slack in the circulatory system caused by the lost blood. Indeed, even after as much as 20 percent of the total blood volume has been lost, the circulatory system often functions almost normally because of this variable reservoir function of the veins(John E. Hall et al 2006).

2.2.6 Specific Blood Reservoirs

Certain portions of the circulatory system are so extensive and/or so compliant that they are called “specific blood reservoirs.” These reservoirs include (1) the spleen, which sometimes can decrease in size sufficiently to release as much as 100 milliliters of blood into other areas of the circulation; (2) the liver, the sinuses of which can release several hundred milliliters of blood into the remainder of the circulation; (3) the large abdominal veins, which can contribute as much as 300 milliliters; and (4) the venous plexus beneath the skin, which also can contribute several hundred milliliters. The heart and the lungs, although not parts of the systemic venous reservoir system, may also be considered blood reservoirs. The heart, for instance, shrinks during sympathetic stimulation and in this way can contribute some 50 to 100 milliliters of blood; the lungs can contribute another 100 to 200 milliliters when the pulmonary pressures decrease to low values (John E. Hall et al 2006).

The spleen as a reservoir for storing red blood cells shows that the spleen has two separate areas for storing blood: the venous sinuses and the pulp. The sinuses can swell the same as any other part of the venous system and store whole blood. In the splenic pulp, the capillaries are so permeable that whole blood, including the red blood cells, oozes through the capillary walls into a trabecular mesh, forming the red pulp. The red cells are trapped by the trabeculae, while the plasma flows on into the venous sinuses and then into the general circulation. As a consequence, the red pulp of the spleen is a special reservoir that contains large quantities of concentrated red blood cells. These concentrated red blood cells can then be expelled into the general circulation whenever the sympathetic nervous system becomes excited and causes the spleen and its vessels to contract. As much as 50 milliliters of concentrated red blood cells can be released into the circulation, raising the hematocrit 1 to 2 percent (John E. Hall et al 2006).

Unit IV The Circulation In other areas of the splenic pulp are islands of white blood cells, which collectively are called the white pulp. Here lymphoid cells are manufactured that are similar to those manufactured in the lymph nodes.

2.3 Pathology

2.3.1 Gross Description

Permission was granted for a complete autopsy. The heart weighed 600 g. The pericardial sac had minimal amount of serous fluid. The pericardium and epicardium were smooth and glistening. The atria were of normal size and free of thrombi. The foramen ovale was closed. The left ventricle was hypertrophic (wall thickness 2cm) and the right ventricle showed severe dilatation and hypertrophy. The valves were partially calcified. The tricuspid valve was hemorrhagic. The postero-lateral papillary muscle of the left ventricle was ruptured with consequent prolapse of the mitral valve (diameter of the ring 11.5 cm). (Figure 4) The chordae tendineae were focally thickened. The myocardium was red-brown with average consistency, and the endocardium was thin and shiny(Thomas D. Boyer 2006).

Examination of the coronary arteries showed complete occlusion of the right coronary artery as well as acute thrombosis of the left circumflex artery. The aorta showed severe atherosclerosis with thrombi and ulceration, especially in the thoracic and abdominal portions. The major branches were unremarkable except for aneurysmal dilatation of the right iliac artery(Thomas D. Boyer 2006).

The lungs were heavy (2250 g combined), but no discrete lesions were identified. The liver was congested (1530 g). Other significant findings included severe nephrosclerosis with cyst formation, and hemorrhagic adrenals, pancreas and intestine. The brain weighed 1255 g and was grossly unremarkable except for severe atherosclerosis of the circle of Willis.

Sudden onset of abdominal pain in a patient that is receiving anticoagulant therapy should alert the clinician of the possibility of bleeding. Potential sources include a gastric or duodenal peptic ulcer, hemorrhagic pancreatitis, and a dissecting or ruptured abdominal aortic aneurysm. Upper GI bleeding was unlikely in the absence of hematemesis or melena. Acute pancreatitis is associated with leukocytosis, but there was no evidence of increased levels of serum amylase and lipase. Abdominal aortic aneurysms are common in patients with atherosclerosis and hypertension. These patients often develop saccular dilatations below the renal and above the iliac arteries(Thomas D. Boyer 2006).

Aortic dissection can occur in patients with a history of hypertension, but are rare in the context of severe atherosclerosis due to the protective effect of substantial medial scarring and fibrosis. Rupture of an aortic aneurysm can cause excruciating pain, but this is a catastrophic event with massive blood loss and rapid death. There is no time for development of progressive pain with subsequent radiation to the hip and dropping hematocrit within a 48 hours period, unless the aneurysm was leaking slowly. Bleeding within a third space (pleura, pericardium and retroperitoneum) has been reported following anticoagulant therapy, although fatal bleeding is rare. Pleural and pericardial hemorrhages usually cause chest pain. Patients with a large pericardial effusion present with symptoms of cardiac tamponade. Dysphagia and dyspnea may result from esophageal or lung compression due to mediastinal or pleural hemorrhage(Thomas D. Boyer 2006).

Retroperitoneal hematomas are more likely to cause abdominal pain that radiates to the extremities. Pain in the hip and leg are the result of entrapment of the lumbar plexus and common femoral nerve, and the dissection of the planes of the psoas muscle. The retroperitoneum is a relatively large and expansible space that allows a gradual accumulation of blood and changes in

the hematocrit values. Retroperitoneal hematomas may occur even with controlled prothrombin time (PT) and partial thromboplastin time (PTT) values; therefore a CT scan is indicated if the patient develops abdominal pain associated with progressive normochromic, normocytic anemia. In this case, the bleeding was most likely caused by heparin rather than by TPA. The adverse effects of TPA are evident early after administration and include stroke, intracerebral hemorrhages and less often, bleeding from vascular access sites. Therapeutic heparin dose has been associated with an estimated bleeding risk of 5%. The risk increases if the dose is given intermittently rather than continuously, and in patients with chronic illnesses such as pulmonary or liver diseases. Interestingly, our patient was a heavy smoker with both severe COPD and evolving cirrhosis. Nonetheless, he had enough spared and functional liver parenchyma to maintain normal coagulation and unremarkable levels of bilirubin and alkaline phosphatase. The sudden onset of shortness of breath was due to the extension of the hemorrhage into the left diaphragmatic region. The cause of death in this case was most likely hypoxemia followed by a cardiac arrhythmia(Thomas D. Boyer 2006).

The patient continued to vomit, the bloody diarrhea persisted and the bowel sounds diminished. Infection or ischemic bowel disease were the clinical diagnoses considered. An abdominal CT-scan showed occlusion consistent with thrombus in the superior mesenteric artery (SMA), which was confirmed by angiography. Thrombectomy of the SMA and Goretex patch angioplasty were performed. In addition, the patient was transfused. Soon after surgery, acute renal failure developed. Hemodialysis and anticoagulation therapy were started. However, 10 days later she had an episode of gastrointestinal bleeding and the heparin was discontinued. The following day the blood pressure suddenly dropped and the patient expired(Thomas D. Boyer 2006).

2.3.2 Gross Description

The heart weighed 500 g and showed dilatation of the right and left atria, and hypertrophy of the left ventricle (1.6 cm in thickness). The tricuspid valve measured 12.6 cm in length. The coronary arteries were partially occluded (60–90%) by atherosclerosis with calcification. The aorta had moderate atherosclerosis. The lungs were congested (850 g combined). Two ulcers were noted in the body of the stomach, each measuring 1 cm in diameter. The distal portion of the jejunum and the proximal portion of the ileum had serosal purple discoloration consistent with ischemic bowel disease. The luminal content was bloody. The vascular graft of the superior mesenteric artery was partially occluded by a thromboembolus. The kidneys weighed 450 g combined and had a finely granular surface. The cut surface was unremarkable(Thomas D. Boyer 2006).

2.3.3 Microscopic Description

The cardiovascular examination confirmed right and left ventricular hypertrophy with mild perivascular fibrosis and multifocal interstitial and replacement fibrosis. Sections from the superior mesenteric artery and its branches revealed medial calcific sclerosis (Monckeberg's) with recent hemorrhage in the portion where fragments of synthetic graft were identified, The lumen was 60% occluded by a hyaline plaque showing signs of remote and recent hemorrhage.

Sections from the lung revealed congestion as well as numerous hemosiderin-laden macrophages, the so called 'heart failure cells', and signs of mild pulmonary hypertension. The small bowel had segments of transmural ischemic and hemorrhagic infarction with focal areas of mucosal regeneration. The kidneys exhibited areas of nodular and diffuse glomerulosclerosis (Kimmelstiel-Wilson). The central nervous system revealed acute hippocampal hypoxic and degenerative changes. The remaining organs were unremarkable; except for the liver which showed mild steatosis and centrilobular congestion(Thomas D. Boyer 2006).

2.3.4 Portal Vein:

The major condition affecting the portal venous system is cirrhosis with portal hypertension (see Cirrhosis). Pylephlebitis refers to inflammation affecting the major portal vein and/or its branches (Figure 13-48) and is seen in association with intra-abdominal suppurative processes such as perforated ulcers, or appendiceal rupture in appendicitis. The most common cause of portal vein thrombosis is cirrhosis (Thomas D. Boyer 2006).

2.3.5 Hepatic Veins and Inferior Vena Cava:

Budd–Chiari syndrome 65–68 refers to obstruction of venous outflow from the liver owing to thrombosis or obstruction of the major hepatic veins and/ or inferior vena cava. Prothrombotic disorders and oral contraceptive use are the most common etiologic factors. The liver shows centrilobular sinusoidal dilatation and congestion (Figure 13-49). Prolonged venous outflow obstruction may result in perisinusoidal fibrosis in centrilobular regions, with bridging fibrosis to Central veins or to portal tracts, and eventually cirrhosis.

Venous outflow obstruction combined with regions of arterial hyperperfusion may stimulate regenerative hyperplasia, evident as nodular.

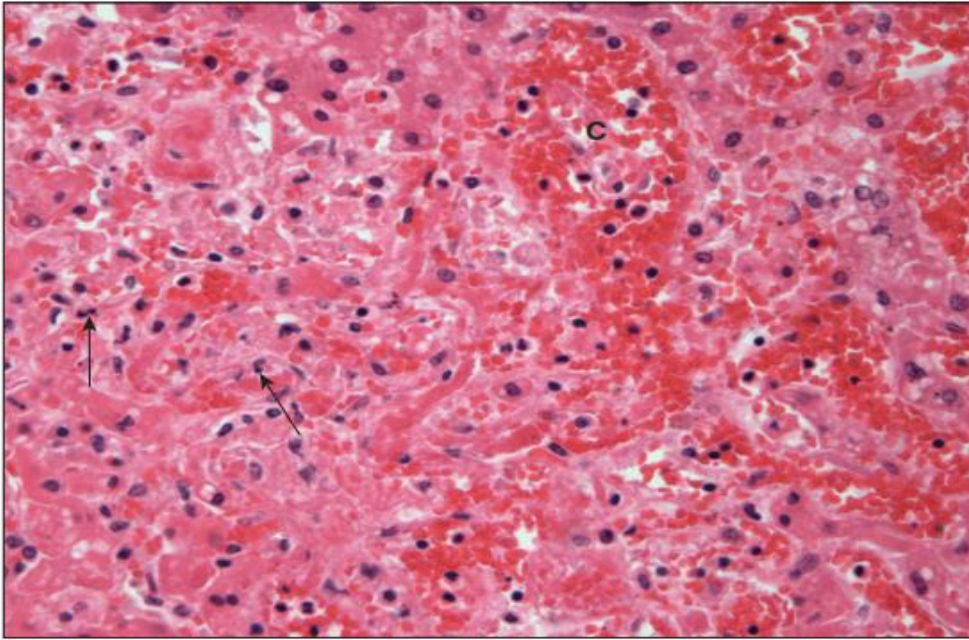


Fig 2.8 Ischemic hepatitis, this postmortem specimen shows a central vein (C) and surrounding congested parenchyma from a patient who died in cardiac failure.

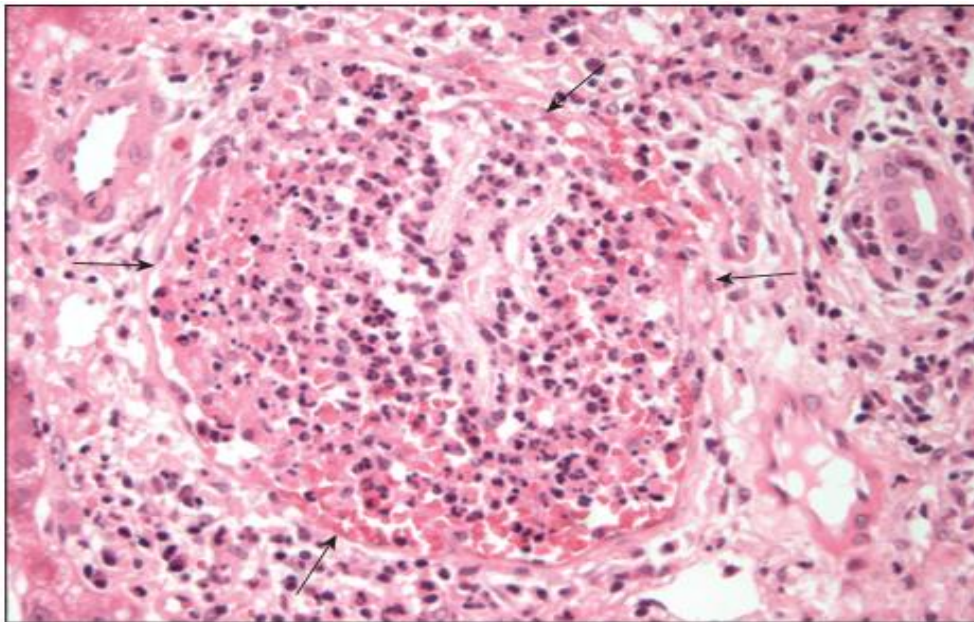


Fig 2.9 pylephlebitis , the portal vein branch outlined by the arrows contains neutrophils and supportive debris

regenerative hyperplasia (to be distinguished from cirrhosis, in which regenerative nodules are surrounded diffusely by cirrhosis), or as solitary or multiple nodules resembling focal nodular hyperplasia (see Tumors and tumor-like lesions). Congenital webs of the inferior vena cava are a rare cause of Budd–Chiari syndrome.

2.4 Angiography:

2.4.1 Multidetector-Row CT Angiography Technique:

CT angiography (CTA) exam has to be performed by using a 64-row scanner before and during infusion of contrast medium (370-400 mgI/ml). Patients were in the supine position with their feet first. A thick-slice pre-contrast acquisition must always be performed to reveal calcifications and to plan the following contrast-enhanced examination, by selecting the volume of acquisition and placing a region of interest in the aorta at the level of the aortic arch. Thin-slice arterial-enhanced images are obtained from 2 cm above the origin of renal arteries to the ankle. CTA-acquisition protocol parameters are the following: 0.625x64mm collimation, 0.7-second gantry rotation, pitch 0.9; scan duration ranged between 18 and 25 seconds (R. Lezzi et al 2003).

Contrast-enhanced images are obtained during bolus intravenous injection of 80-120 ml of a high-concentration iodinated non-ionic contrast medium (370-400mgI/mL) + 40mL of saline solution, administered with an automated injector at a flow rate of 4 ml/s via an antecubital vein.

A very important achievement in CT-angiography is the optimal contrast-medium dynamic. As a matter of fact, scanning should start when the examined structures have reached an ideal level of opacification; therefore, scan delay has to be individualized per patient, using bolus-tracking software. However, with the increased speed of the new scanner generation (until 90 mm/sec possible with a 64-detector row scanners), if the CT data acquisition is initiated at the time of contrast medium bolus arrival in the aorta, the CT acquisition may outpace the bolus, with resultant inadequate opacification of arteries, to avoid this problem, we suggest to decrease the table speed

(until to 30mm/sec) increasing the scanning delay by selecting an appropriate "diagnostic delay" (interval of time between automated detection of the contrast medium bolus arrival within the target vessel and the real initiation of the CT angiographic data acquisition) (R.Lezzi et al 2003). Our contrast-medium injection protocol suggest to use a bolus-tracking software capturing 150 HU on the abdominal aorta, at the level of the celiac trunk, to trigger scanning and ensure a correct peak enhancement, by adding a diagnostic delay of 8 seconds in order to avoid to outpace the bolus. In a limited number of patients with large aorto-iliac and femoro-popliteal aneurysms, an optional second acquisition (from the knees to the feet) should be preprogrammed and initiated immediately after the first acquisition if reconstructions of the initially acquired CT data show no opacification of the distal arteries (R.Lezzi et al 2003).

CTA examination must be complemented by postprocessing reconstructions, including maximum-intensity projection (MIP), curvilinear reformation (CVR) and volume rendering (VR).

2.4.2 Normal Anatomy

Normal anatomy of peripheral system on axial and reconstructed-3D images is described and compared with anatomical and angiographic images.

2.4.3 Steno-Obstructive Disease

Peripheral occlusive artery disease () is estimated to be present in 1.4 to 1.9% of people at the age of 40-49 years, in 6.9% of people at the age of 50-59 years, and in 20% of people over 70 years. Critical limb ischemia has a mortality rate of 46% at 5 years and a percentage of 27% of amputations at 1 year. However, revascularization strategies including surgical and endovascular procedures guarantees success in terms of functional recovery of the ill limb, as well as in terms of duration in time. Clinical evaluation and accurate and timely diagnostic work-up are mandatory

in order to assess the morphological and functional features of the lesion to establish the appropriate therapeutic approach (medical/ surgical/ endovascular therapy).

CTA is a highly accurate and precise technique for determining the degree and the length of stenosis. Initially, all images should be reviewed in the axial plane. 3D-images are always helpful. The degree of stenosis is generally calculated according to criteria developed by the European Carotid Surgery Trial (ECST): measurements are made across the lumen through the narrowest portion compared to the original arterial outline. The degree of stenosis is reported as a percentage of stenosis: I: normal; II (1%-29%): mild; III (30%-69%): moderate; IV (70%-99%): severe. Lesions may be smooth, irregular, or focal, or they may involve a long segment. Special consideration must be given for critical degrees of stenosis, often termed the "string sign". The presence of contrast agent in a markedly restricted lumen may be an indication of a critical proximal focal stenosis or longer segmental narrowing. Indirect signs of significant stenosis are represented by the presence of post-stenotic focal vessel dilation (reversible post-stenotic ectasia) as well as by the uniform vessel lumen reduction below the stenosis, indicative of a flux reduction. CTA is also the best modality for analyzing plaque morphology because it allows visualization of the atheromatous plaque. There are three types of plaque: soft plaques, that shows a mean density of 14 ± 26 HU (ranging from -42 to +47 HU), intermediate plaques, that shows a mean density of 91 ± 21 HU (ranging from 61 to 112 HU), and calcified plaques, that shows a mean density of 419 ± 194 HU (ranging from 126 to 736 HU). Detection of ulcerated plaques may prove to be mandatory, since it has been suggested that the presence of plaque ulceration is a risk factor for embolism.

CT sign of ulcerated plaques on axial images is represented by an intraluminal linear contrast material filling defect which has to be differentiated by intimal flap/dissection. False-positive

results are related to motion artifacts. Sudden movement, breathing, or swallowing by the patient during scanning may result in a misregistration of the axial images on 3D or multiplanar reformatted images. Principal limitation of CTA are represented by the presence of diffuse cuff calcifications in the smaller arterial branches of lower limbs which enable an accurate definition/grading of steno-obstructive lesions (R.Lezzi et al 2003).

2.4.4 Aneurysmal Disease

Aneurysmal pathology is a local, irreversible, vascular caliber increasing over 50% of the previous and next tract. They are usually found during the 6th and 7th decades of life and have a strong male predilection with a prevalence of 2% in population and 5% in population >65 years old.

Aneurysms are classified with regards: istopathology; morphology; etiology; location.

Istopathological classification divides aneurysm in true and false according to the complete or not interesting of all arterial wall layers. They are also divided in terms of morphological aspect into sacciform and fusiform depending of complete or not involvement of the vascular circumference.

Aneurysms may rarely be associated with connective tissue diseases such as Marfan syndrome or Ehlers-Danlos syndrome or, even more rarely, with pregnancy. Almost all true aneurysms are non-specific. Historically, the nonspecific form of aneurysmal disease that affects the abdominal aorta and the iliac common femoral, and popliteal arteries has been described as "atherosclerotic".

Risk factors associated with atherosclerotic disease are also associated with non-specific aneurysms. However, atherosclerotic disease and these risk factors incompletely define the cause of these aneurysms, which appears to be multifactorial. Finally they are classified in: central (aortic), visceral (splancnic and renal) and peripheral (cervical and of limbs). 80% of aneurysm involves aortic wall under the emerging of the renal branches; 25% of them involve the iliac bifurcation too. Popliteal aneurysms (PAAs) are the most common peripheral aneurysms (PAAs).

PAAAs are associated with aneurysms in other locations and are bilateral in 50%-70% of cases; as a matter of fact, in patients with a PAA, it is mandatory to look for Abdominal Aortic Aneurysm and/or a contralateral PAA.

Many patients with popliteal aneurysms are asymptomatic at the time of diagnosis; symptomatic patients can present with a lower-extremity ischemia, which can manifest as claudication, rest pain, or severe ischemia associated with thrombosis or embolization. As a matter of fact, patients with popliteal aneurysms have a risk of limb-threatening thrombotic complications, with embolization and above all rupture, with an incidence of 18-31% .

CTA allows identification of the aneurysm and differential diagnosis from ectasia (caliber increasing less than 50%), the description of the lesion, evaluating location, length, extension, transverse diameter (valuated always perpendicularly to major vascular board), presence of calcifications and location of thrombotic apposition (concentric/ eccentric) measuring its maximum thickness, evaluating the look of its edges and excluding the possible presence of iperdensity that can suggest an instable nature of the thrombus.

3D-images are particularly useful in planning surgical/endovascular treatments, demonstrating the degree of extension of the aneurysm in the coronal and sagittal planes and the relationship between the aneurysm and the adjacent structures.

CTA allows direct visualization of the stent struts and lumen and this is fundamental for a more reliable assessment of in-stent patency because distal run-off cannot be considered a reliable indicator of it, because contrast material can fill of the peripheral artery distal to the stent via collateral arteries, which may obscure the real pathologic lesion inside the stent.

The stent may be considered to be occluded if the lumen inside the device appears darker than the contrast-enhanced vessel lumen proximal to the stent. Nonocclusive in-stent neointimal

hyperplasia is characterized by the presence of a darker rim between the stent and the contrast-enhanced vessel lumen and is secondary to the healing response to procedure-related vessel injury. If neointimal hyperplasia exceeds a luminal diameter reduction of 50%, the process is consistent with hemodynamically significant in-stent restenosis.

In the post-PTA follow-up, it has to be evaluated the patency or restenosis/occlusion of treated vessel, looking for procedural complications, as well as intimal dissection, vessel rupture and/or distal embolization (R.Lezzi et al 2003).

2.4.5 Traumatic Lesions

Diagnostic queries concerning acute vascular disorders involving the arteries of the lower limbs are not very common, but have a significant clinical impact. An early diagnosis together with an accurate and detailed morphological and functional assessment of the involved arterial area is necessary to select the most appropriate treatment and give the patient the best chances of success. In the last few years many studies have compared MSCT angiography to DSA for the assessment of patients with peripheral arteriopathy involving the lower limbs, with an excellent concordance between the two methods.

Traumatic arterial lesions are classified as a partial or complete obstruction (rapid change in caliber or loss of opacification of vessels), arterial laceration (spreading of contrast medium), pseudoaneurysm (extravascular collection of contrast medium), arteriovenous fistula (early opacification of venous structures), or intimal flap (intraluminal linear contrast material filling defect).

A limitation of MDCT angiography can be the possible presence of streak artifacts due to metal bodies in the event of penetrating traumas that may render the CT angiogram uninterpretable.

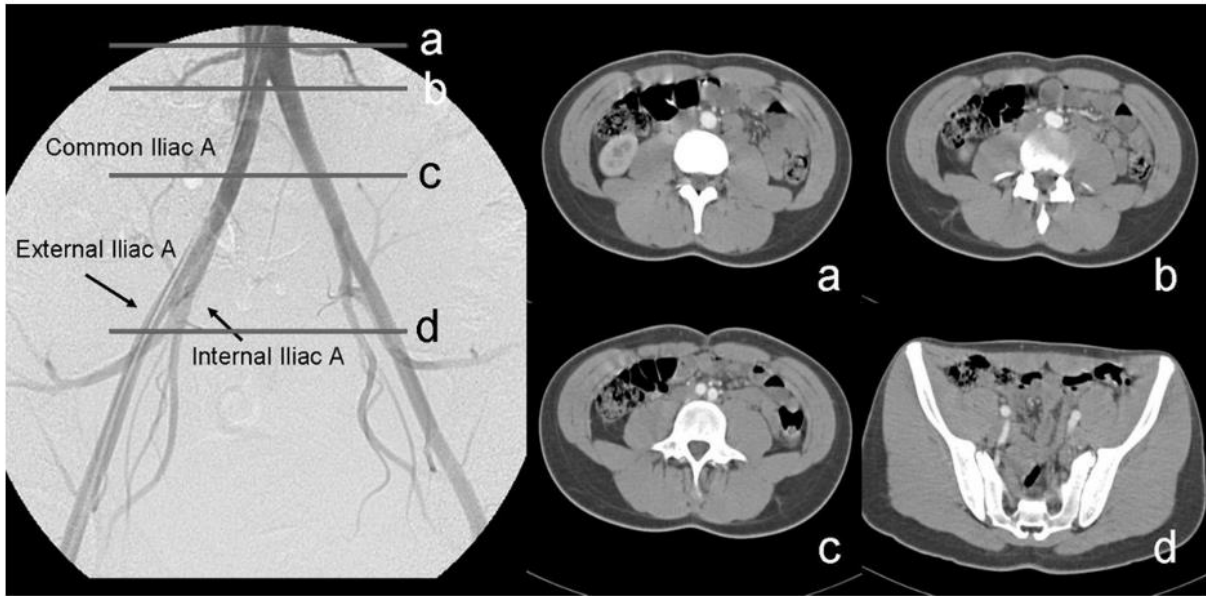


Fig. 2.10: Anatomy: aorto-iliac district. Axial images obtained at the level of abdominal aorta (a), aortic bifurcation (b), common iliac arteries (c), and external and internal iliac arteries (d)

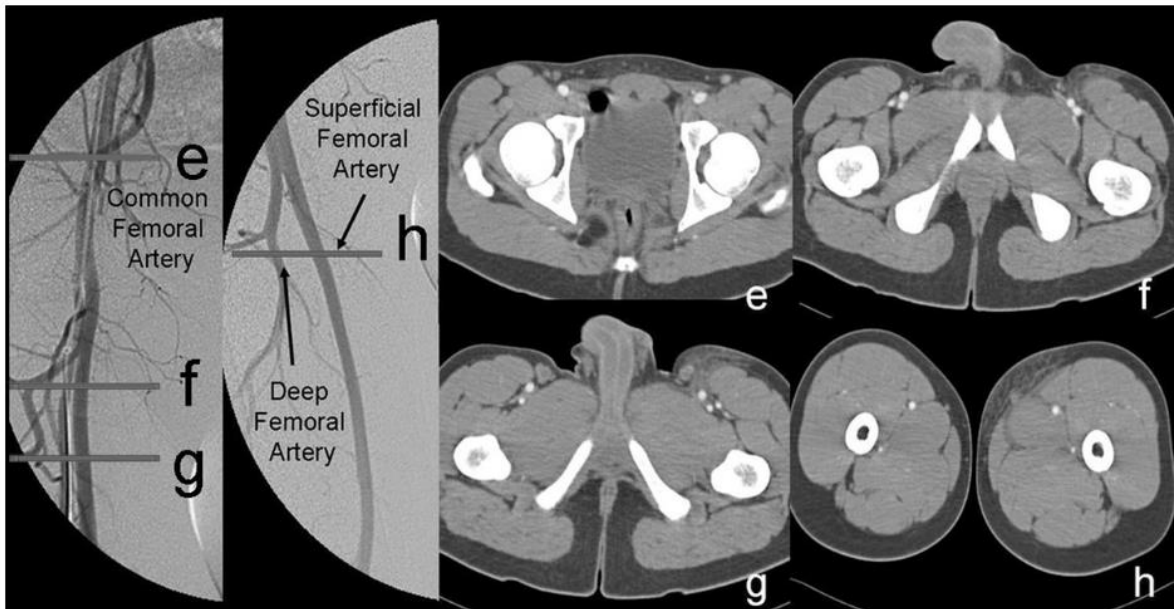


Fig. 2.11: Anatomy: femoro-popliteal district. Axial images obtained at the level of common femoral artery (e), common femoral bifurcation (f-h).

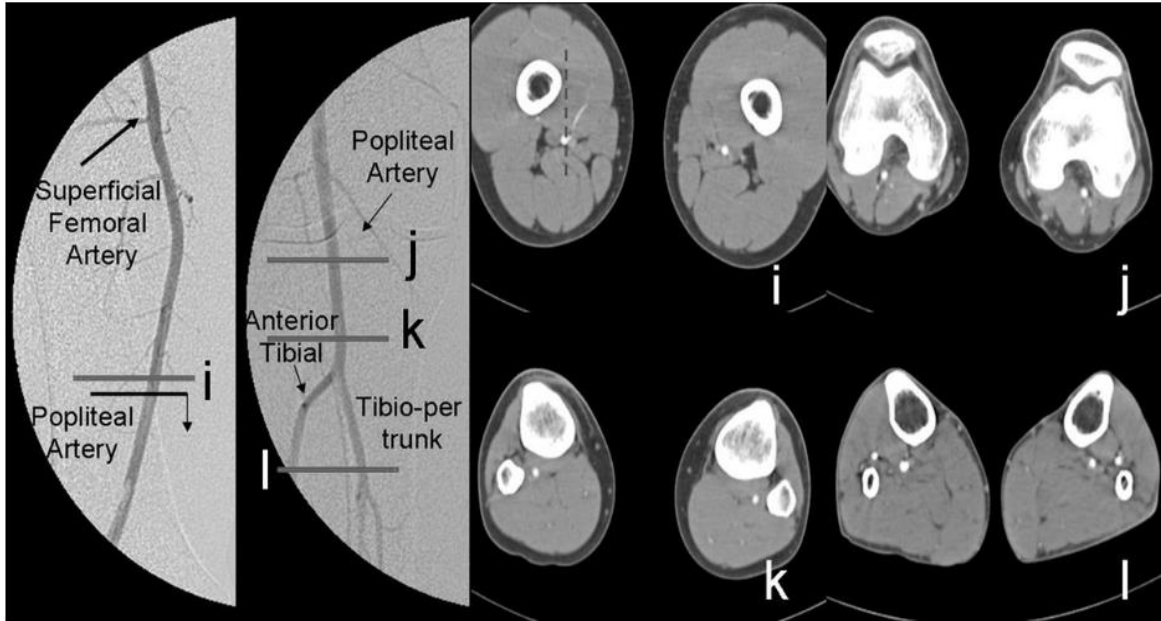


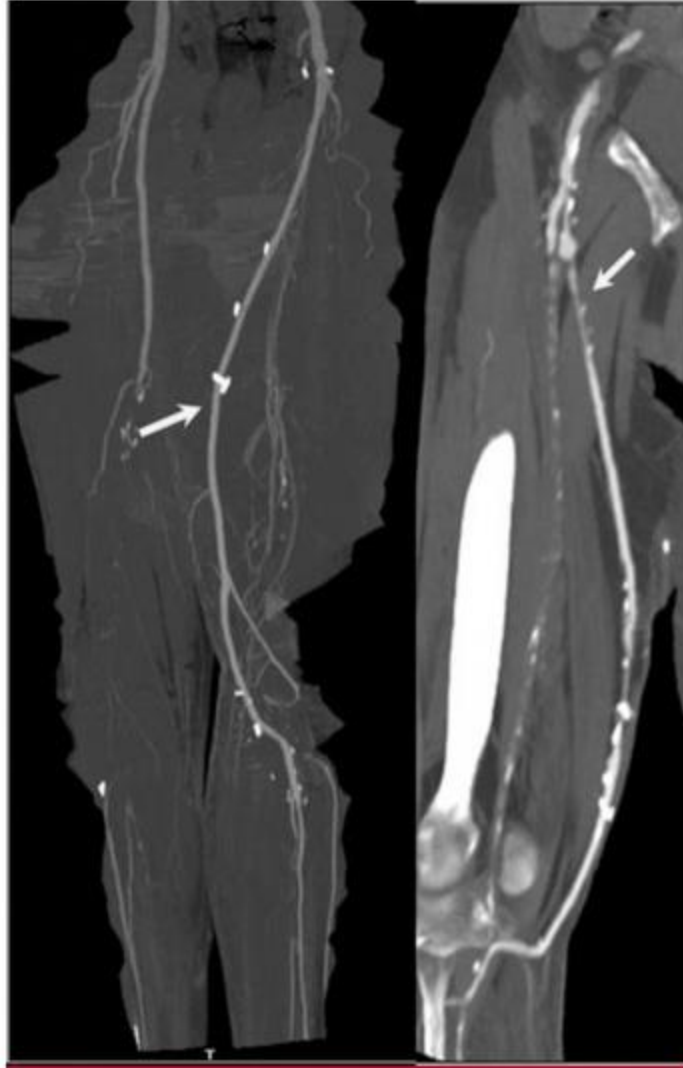
Fig. 2.12: Anatomy: popliteal-infrapopliteal district. Axial images obtained at the level of proximal popliteal artery (i), popliteal artery (j), distal popliteal artery (k), and anterior tibial artery and tibio-peroneal trunk (l)



Fig. 2.13: Anatomy: Aorto-iliac district. MIP- and VRT-images.



Fig. 2.16: MIP- and VRT-images: steno-obstructive disease



*Fig. 2.17: MIP-images: Femoro-popliteal bypass with a venous conduct: nonligated venous
Branches*

2.4.6 Multi Detector Computed Tomography (MDCT)

Over more than 30 years of advances in technologies, including x-ray generation, filtration design, detector, firmware, and post-processing, CT has developed into a medical imaging modality with the capability of obtaining excellent resolution for both high contrast and low contrast tasks, as well as the capability to perform volumetric imaging by the implementation of multi-row detectors (MDCT). It has been a major diagnostic tool and has been impacting patient healthcare throughout

the entire world. Today CT is routinely used as a key component in Radiology and Oncology departments for many areas of medical applications. To name a few, within Radiology department, it is used in head scans to detect infarction, hemorrhage, or trauma; it is used in thoracic scans for detecting both acute and chronic changes in the lung parenchyma; it is used in Cardiology to diagnose cardiovascular diseases; it is used in abdomen or pelvic scans to determine the stage of cancer and to follow progress; it is also used in extremity scans to image complex fractures, especially one around joints because of its ultra-high spatial resolution. Within Oncology department, CT is used to obtain attenuation properties for body tissues in order to perform necessary calculations of radiation dose distribution in treatment planning (Mettler, F.A et al 2008).

CT scanners use x-ray tubes to generation photons. In this process, electrons are emitted from cathode via thermionic emission and are accelerated within the tube towards anode driven by the potential difference between the cathode and the anode. The highly energetic electrons then interact with matter (usually tungsten) and convert their kinetic energy into heat and electromagnetic radiation (photons) through the process of bremsstrahlung. Figure 1 shows the physical look of the anode. The fluence of photons depends on kVp and mAs. kVp is defined as the peak tube potential between the cathode and the anode. It determines the highest energy of photons within the beam. mAs is the multiplication of tube current (the rate of the charge of electrons from the cathode to the anode) and exposure time. mAs is proportional to the fluence of the x-ray beam (Mettler, F.A et al 2008).

During the CT scan a patient lies on the table while the x-ray tube and the detector ring spin in the gantry in a very fast speed (as fast as 0.27s/rotation for certain manufacturer). Fan shaped beams are used in modern CT scanners as shown in figure 2. There are two different scan modes with

respect to the pattern of the movement of the bed: axial scan and helical scan. In axial scan, the bed moves incrementally after every rotation so the anatomy is captured section by section; in helical scan, the bed moves continuously while the tube and detector are rotating.

Under helical scan mode, pitch is defined as the advance of the table in a rotation divided by the nominal collimation width in z direction. Helical scan was introduced in 1990s and it has dramatically increased the time efficiency of CT scans.

The number of CT scans in United States has increase from 18.3 million in 1993 to 62.0 million in 2006, with an estimated annual growth rate of 10% 5,6 . Especially since the introduction of MDCT in mid 1990s, the use of CT has increased dramatically due to its improved capacity. In clinical practice, CT exams consists 15% of the total number of radiological imaging procedures, but it contributes to 50% of the population radiation exposure from medical procedures, and it contributes to 25% of the population radiation exposure from all sources, including background radiation. This has lead to concerns about the potential risks of radiation hazards to patients (Mettler, F.A 2008).

Imaging is basically a process consisting of two distinct stages: image recording and image display (Wagner 1983, ICRU 1996). This division is especially important in digital imaging, where these stages are clearly separate. In digital imaging the image recording stage (or the image data stage) determines the information that has been captured in the image data and can be analysed in terms of the pixel values. Performing actual physical measurements of the display stage is cumbersome and its evaluation is for the most part done mainly visually.

2.5 Previous Study:

Karen Visser, 2000 The aim of this study is To summarize and compare the published data on gadolinium-enhanced magnetic resonance (MR) angiography and color-guided duplex ultrasonography (US) for the work-up for peripheral arterial disease.

Materials and Methods: Studies published between January 1984 and November 1998 were included if (a) gadolinium-enhanced MR angiography and/or color-guided duplex US were performed for evaluation of arterial stenoses and occlusions in the work-up for peripheral arterial disease of the lower extremities, (b) conventional angiography was the reference standard, and (c) absolute numbers of true-positive, false-negative, true-negative, and false-positive results were available or derivable.

Results: With a random effects model, pooled sensitivity for MR angiography (97.5% [95% CI: 95.7%, 99.3%]) was higher than that for duplex US (87.6% [95% CI: 84.4%, 90.8%]). Pooled specificities were similar: 96.2% (95% CI: 94.4%, 97.9%) for MR angiography and 94.7% (95% CI: 93.2%, 96.2%) for duplex US.

Summary receiver operating characteristic analysis demonstrated better discriminatory power for MR angiography than for duplex US. Regression coefficients for MR angiography versus US were 1.67 (95% CI: 20.23, 3.56) with adjustment for covariates, 2.11 (95% CI: 0.12, 4.09) without such adjustment, and 1.73 (95% CI: 0.44, 3.02) with a random effects model.

Conclusion: Gadolinium-enhanced MR angiography has better discriminatory power than does color-guided duplex US and is a highly sensitive and specific method, as compared with conventional angiography, for the work-up for peripheral arterial disease.

Dominik Fleischmann et al 2006 studied Lower-extremity computed tomographic (CT) angiography (ie, peripheral CT angiography) is increasingly used to evaluate patients with

peripheral arterial disease. It is therefore increasingly important for all vascular specialists to become familiar with the strengths and limitations of this new technique. The aims of this review are to explain the principles of scanning and injection technique for a wide range of CT scanners, to explain and illustrate the properties of current image postprocessing tools for effective visualization and treatment planning, and to provide an overview of current clinical applications of peripheral CT angiography.

T. Laswed et al, 2008 evaluated 16-detector-row CT in the assessment of occlusive peripheral arterial disease (PAD) of the abdominal aorta and lower extremities using an adaptive method of acquisition to optimise arterial enhancement especially for the distal foot arteries. Thirty-four patients underwent transcatheter angiography (TCA) and CT angiography within 15 days. For each patient, table speed and rotation were selected according to the calculated optimal transit time of contrast material obtained after a single bolus test and two dynamic acquisitions at aorta and popliteal arteries. Analysis included image quality and detection of stenosis equal or greater than 50% on a patient basis and on an arterial segment basis. Sensitivity and specificity of CT were calculated with the TCA considered as the standard of reference. CT was conclusive in all segments with no technical failures even in difficult cases with occluded bypasses and aneurysms. On patient-basis analysis, the overall sensitivity and specificity to detect significant stenosis greater than 50% were both 100%. Segmental analysis shows high values of sensitivity and specificity ranging from 91 to 100% and from 81 to 100%, respectively, including distal pedal arteries. Sixteen-detector-row CT angiography using an adaptive acquisition

improves the image quality and provides a reliable non-invasive technique to assess occlusive peripheral arterial disease, including distal foot arteries.

Marc et al 2007 studied the multi-detector row computed tomography (MDCT), scan speed and image quality has improved considerably. Since the longitudinal coverage is no longer a limitation, multi-detector row computed tomography angiography (MDCTA) is increasingly used to depict the peripheral arterial

runoff. Hence, it is important to know the advantages and limitations of this new non-invasive alternative for the reference test, digital subtraction angiography. Optimization of the acquisition parameters and the contrast delivery is important to achieve a reliable enhancement of the entire arterial runoff in patients with peripheral arterial disease (PAD) using fast CT scanners. The purpose of this review is to discuss the different scanning and injection protocols using 4-, 16-, and 64-detector row CT scanners, to propose effective methods to evaluate and to present large data sets, to discuss its clinical value and major limitations, and to review the literature on the validity, reliability, and cost-effectiveness of multi-detector row CT in the evaluation of PAD.

Edwards et al 2005 assess whether multi-detector CT angiograms (MDCTA) of the lower limb arteries, compared with conventional digital subtraction angiograms (DSA), could replace invasive arteriography in patients with symptomatic peripheral arterial disease.

Materials and Methods: In a prospective comparative analysis of MDCTA and DSA in 44 patients, MDCTA was analyzed using volume-rendered images acquired at a workstation and viewed in tandem with the original axial data. Designated arterial segments were graded according to their degree of stenosis.

RESULTS: We found agreement for the degree of stenosis in 88.8% and 85.4% of 1024 segments analysed for two observers. The sensitivity for treatable lesions (>50% stenosis) was 79.1% and 72% with a specificity of 93.3% and 92.6%. DSA failed to visualize 7.3% of segments that were visible with MDCTA. These segments were exclusively downstream to long segment occlusions.

Conclusion: medical using 4-slice machines is insensitive to detecting significant arterial stenoses in the lower limb arteries. MDCTA is superior to DSA in its visualization of arterial territories downstream to significant occlusive disease.

Thomas Sandgren et al 1999 aimed to determine the relevance of dilatations of the common femoral artery (CFA), knowledge of the normal CFA diameter is essential. The diameter of the CFA in healthy male and female subjects of different ages was investigated.

8 to 81 years of age) with echo-tracking B-mode ultrasound scan. The influence of age, sex, height, weight, body surface area (BSA), and systolic blood pressure was analyzed by means of a multiple regression model.

Results: The CFA increased steadily in diameter throughout life. From 25 years onwards, the diameter was larger in men than in women. Significant correlations were found between the CFA diameter and weight ($r = 0.58$ and $r = 0.57$ in male and female subjects, respectively; $P < .0001$), height ($r = 0.49$ and $r = 0.54$ in male and female subjects, respectively; $P < .0001$), and BSA ($r = 0.60$ and $r = 0.62$ in male and female subjects, respectively; $P < .0001$). Age and BSA were used to create a model for prediction of the CFA diameter ($r = 0.71$ and $r = 0.77$ in male and female subjects, respectively; $P < .0001$).

Conclusion: The diameter of the CFA increases with age, initially during growth but also in adults. This is related to age, body size, and sex—male subjects have larger arteries than female subjects.

It is now possible to predict the normal CFA diameter, and nomograms that may be used in the study of aneurysmal disease are presented.

T. Lanne et al 2000, Objectives To study 40-55 mm aneurysms and calculate their size in relation to the individual predicted normal aortic diameter to see if this might add anything in the evaluation of treatment.

Material and methods: The anteroposterior diameter of 40-55 ,mm AAAs was measured with an echo-tracking ultrasonic technique in 147 consecutive patients. The weight and height were registered and body surface area calculated. The predicted normal aortic diameters were defined according to nomograms and the diameter increase from the predicted normal aortic size in the individual aneurysms calculated.

Results: The median AAA diameter was 48 mm (range 40-55), the BSA 1.85 m² (1.42-2.37), and the predicted AO size 19.4 mm (14.3-21.6). The calculated increase of size in the individual aneurysms was 2.51 (1.9-3.53), that is the spread of data doubled as compared to conventional diameter measurements. When females and males were studied separately the AAA diameter was 46.5 mm (40-55) and 48 mm (40-55), respectively (NS). Since the BSA was significantly lower in women than in men, 1.63 (1.42-1.95) and 1.89 (1.47-2.37), respectively (p<0.0001), also the predicted normal aortic size was lower, 16.4 (14.3-17.8) vs. 19.7 (18.0-21.6) (p<0.0001). Thus, the AAA diameter increase from the predicted size was larger in women than in men; 2.93 (2.25-3.53) vs. 2.46 (1.90-2.94), respectively (p<0.0001).

Conclusion: To define an aneurysm as a localised dilatation of an artery exceeding 50% of the expected normal diameter is now possible. This may facilitate how to treat especially smaller aneurysms and give new information concerning patterns of growth and risk of rupture.

Christy k. Holland et al 1998 aimed this study to establish normal values for volumetric blood flow in the leg at rest using Doppler ultrasound, and to determine what biophysical factors influence resting volumetric flow. Arterial blood flow was measured at four sites in the legs of 40 healthy subjects using an ATL Ultramark 9 HDIt system. All subjects were nonhypertensive nonsmokers with ankle brachial index values greater than 1 and no history of vascular disease. The subjects, 20 of each gender, in age ranging from 20 to 64 y were examined. Blood flow was calculated from the time-averaged, intensity-weighted mean velocity Doppler waveforms and vessel cross-sectional area at the same site. Thigh and calf circumference measurements were used to estimate muscle masses. The mean flow and standard error measured in four arteries in the leg were: 284 6 21 mL/min in the common femoral (CFA); 152 6 10 mL/min in the superficial common femoral (SFA); 72 6 5 mL/min in the popliteal; and 3 6 1 mL/min in the dorsalis pedis. Although women tended to have higher time-averaged mean velocities in the CFA and SFA than men (t-test, $p < 0.008$), their arterial cross-sectional areas tended to be smaller (t-test, $p < 0.004$) and no statistically significant difference was found between men and women in volumetric flow at any site.

No correlation was found between age, weight, height, muscle mass and volumetric flow at all four sites. These estimates of lower extremity volumetric flow in healthy subjects provide a baseline for future studies of flow rates in patients with vascular disease.

Chapter Three

3.1 Material and Methods

3.1.1 Material:

All patients examined on a Helical Multi detector CT scanner scanner (CXXG-012A Toshiba scanner 64 slice, GE Dual slice) in Doctors hospital , Medical Modern Center respectively, used for collecting data from CT Angiography.

The investigation was performed on 300 patients healthy 100 diabetic 100 hypertensive 100 patients

3.1.2 Design of the study

This is a descriptive cross-section study where a representative sample of patient was collected from radiology department at Doctors hospital during the period from June2014 to October 2016.

3.1.3 Population

All patients refer to the hospital for lower limb disease having the characteristics signs and symptoms of lower limb artery disease for the first time i.e. he/she did not receive medication and their age above 40 years.

3.1.4 Sample size and type:

The sample of this study is of a convenient type will consisted of 300 patients suffering from lower limb diseases.

3.1.5 Place and duration of the study:

The study will be conducted in the period from 7/2014 to Octobers 2016 in Khartoum at Doctors hospital and Khartoum Police Hospital.

3.1.6 Method of data collection

Technique

There are no specific pre-scanning preparations necessary for MDCTA of the peripheral arteries. The patient is placed comfortably, in the supine position with raised arms on the CT table. The legs are stabilized with cushions around the legs and slightly strapped with adhesive at distally. It is important that the patient does not wear metal zippers or buttons on their clothing, since this can have a negative influence on the image quality, especially when using postprocessed images. Oral contrast should not be used, as this complicates postprocessing display. Contrast material needs to be administered at body temperature to decrease the viscosity. The protocol can be completely programmed into the scanner.

Technical parameters

The main challenge for peripheral CT angiography is the great range of the vascular system that needs to be depicted. Using a scanogram of approximately 1,500-mm length, the coverage of the acquisition is planned from the celiac trunk (T12 vertebral body) to the level of the talus using 4D-CT, or to the level of the feet using 64D-CT or higher. Scout image with three planned reconstruction batches of the abdomen, the upper legs, and the lower legs to preserve postprocessed image resolution. The frames 3-1, 3-2, and 3-3 depict the field of view of the three data sets.

Scan duration

The optimal scan duration for peripheral CT angiography varies between approximately 20 to 40 second, depending on the number of detector rows and the collimation. The velocity of a contrast bolus to travel from the aorta to the popliteal arteries varies from 29 to 177 mm/s in patients with PAD. This large variability is unpredictable and does not correspond to the severity of PAD. Based on these bolus travel times, it is recommended to limit the maximum table speed on faster scanners to 30 mm/s to avoid outrunning the bolus, leading to poor distal vessel opacification. This can be obtained, for example, by limiting the gantry rotation speed from 0.33 to 0.5 rotations per second or reducing the pitch. Moreover, it is advised to program a second acquisition protocol into the scanner to start immediately if delayed distal enhancement is detected. Because the time of the contrast bolus to travel from the aorta to the ankles varies from 7 to 40 s, a longer scan duration increases the risk of venous contamination, especially when there is critical ischemia and inflammation. Nevertheless, the discrimination of the arteries from the veins is often possible due to the stronger arterial enhancement and the anatomic 3D information.

Contrast injection

It is important in peripheral CT angiography to obtain a high and homogenous enhancement of the arterial tree and to synchronize the acquisition with the enhancement. The optimization of acquisition timing and contrast medium delivery is essential for vascular assessment and image postprocessing. Normally, attenuation values higher than 200 HU in the arteries is considered suitable in MDCTA. For the intravenous injection of contrast medium in the antecubital vein, 22- and 20-gauge intravenous cannulas are needed for the maximal flow rates of 3.5 and 5.0 mL/s, respectively.

3.1.7 Method of data analysis

The data will be analyzed by using Excel and SPSS software under windows by portraying the frequency distribution of the patient with the age, lower arterial limb diseases, and linear association of the age, diabetes and gender with the type of lower limb arterial disease.

Chapter Four

4.1 Results:

Table 4.1 show statistical parameters of measurement the dimensions to abdominal aorta and bifurcation to left and right common femoral artery all patients:

| | Mean | Median | STD | Min | Max |
|-------------|-------|--------|-------|-----|-----|
| Lower Lt | 7.68 | 8 | 1.113 | 5 | 10 |
| Medium Lt | 7.96 | 8 | 1.117 | 5 | 10 |
| Upper Lt | 8.12 | 8 | 1.206 | 5 | 11 |
| Lower Rt | 8.10 | 8 | 1.199 | 5 | 11 |
| Medium Rt | 8.04 | 8 | 1.117 | 5 | 10 |
| Upper Rt | 8.14 | 8 | 1.195 | 6 | 11 |
| Bifurcation | 16.48 | 17 | 1.832 | 12 | 22 |

Table 4.2 measurement of dimensions of abdominal aorta and bifurcation to left and right common femoral artery according to gender:

| | <i>Gender</i> | Mean | Median | STD | Min | Max |
|------------------|---------------|------|--------|-------|-----|-----|
| Lower Lt | <i>Male</i> | 7.78 | 8 | 1.121 | 5 | 310 |
| | <i>Female</i> | 5.57 | 8 | 1.161 | 5 | 10 |
| Medium Lt | <i>Male</i> | 8.07 | 8 | 1.238 | 5 | 10 |
| | <i>Female</i> | 7.83 | 8 | 1.114 | 6 | 10 |
| Upper Lt | <i>Male</i> | 8.41 | 8 | 1.279 | 5 | 11 |
| | <i>Female</i> | 7.78 | 8 | 1.043 | 6 | 10 |
| Lower Rt | <i>Male</i> | 8.33 | 9 | 1.330 | 5 | 11 |
| | <i>Female</i> | 7.83 | 8 | 0.984 | 6 | 10 |
| Medium Rt | <i>Male</i> | 8.33 | 9 | 1.209 | 5 | 10 |
| | <i>Female</i> | 7.70 | 8 | 1.118 | 6 | 10 |
| Upper Rt | <i>Male</i> | 8.59 | 9 | 1.083 | 7 | 11 |
| | <i>Female</i> | 7.61 | 8 | 1.118 | 6 | 10 |

| | | | | | | |
|--------------------|---------------|-------|----|-------|----|----|
| Bifurcation | Male | 16.74 | 17 | 1.810 | 13 | 22 |
| | Female | 16.17 | 16 | 1.850 | 12 | 20 |

Figure 4.1 show compare between mean of left and Right common femoral artery and Bifurcation abdominal aortic

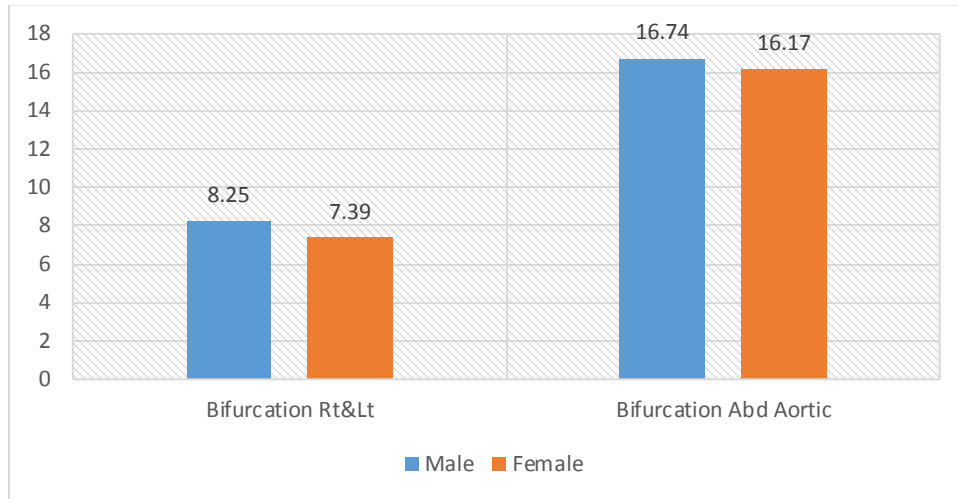


Table 4.3 show independent T-Test of equality means for all measurements

| Independent Samples Test Gender | | |
|---------------------------------|------------------------------|-----------------|
| | t-test for Equality of Means | |
| | T | Sig. (2-tailed) |
| lower_Lt | 1.004 | .320 |
| medium_Lt | 1.041 | .303 |
| upper_Lt | 1.999 | .051 |
| lower_Rt | 1.923 | .060 |
| medium_Rt | 2.038 | .047 |
| upper_Rt | 3.139 | .003 |
| Bifurcation | .953 | .345 |

Table 4.4 show paired sample T-Test for Left and Right measurement of common femoral artery

| Paired Samples Statistics | | | |
|----------------------------------|-----------|-------|-------------------|
| | | Mean | Std. Deviation |
| Pair 1 | lower_Lt | 7.740 | 1.1075 |
| | lower_Rt | 7.992 | 1.1089 |
| Pair 2 | medium_Lt | 7.896 | 1.0662 |
| | medium_Rt | 7.968 | 1.1582 |
| Pair 3 | upper_Lt | 8.078 | 1.1687 |
| | upper_Rt | 8.100 | 1.1101 |

Table 4.5 show paired samples for correlation between Left and Right measurements of common femoral artery

| | | Correlation | Sig. |
|--------|--------------------------|-------------|------|
| Pair 1 | lower_Lt & lower_Rt | .777 | .000 |
| Pair 2 | medium_Lt & medium_Rt | .877 | .000 |
| Pair 3 | upper_Lt & upper_Rt | .663 | .000 |

Table 4.6 show paired samples T-Test for significant 2-tailed of Left and Right measurements common femoral artery

| | | t | Sig. (2-tailed) |
|--------|-----------------------------|--------|-----------------|
| Pair 1 | lower_Lt - lower_Rt | -2.407 | .020 |
| Pair 2 | medium_Lt - medium_Rt | -.911 | .367 |
| Pair 3 | upper_Lt - upper_Rt | -.166 | .869 |

Figure 4.2 show correlation between upper right and upper left common femoral artery

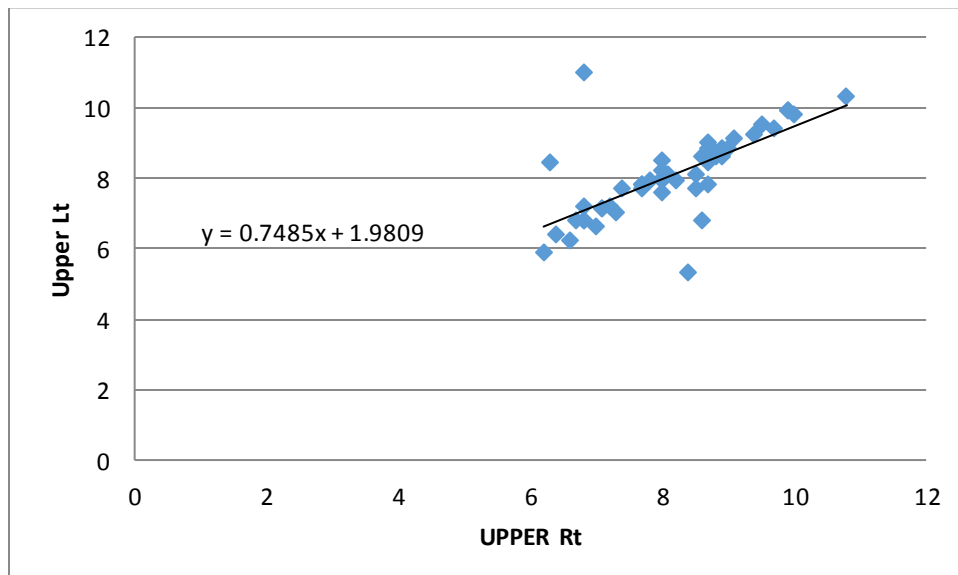


Figure 4.3 show correlation between middle right and middle left common femoral artery

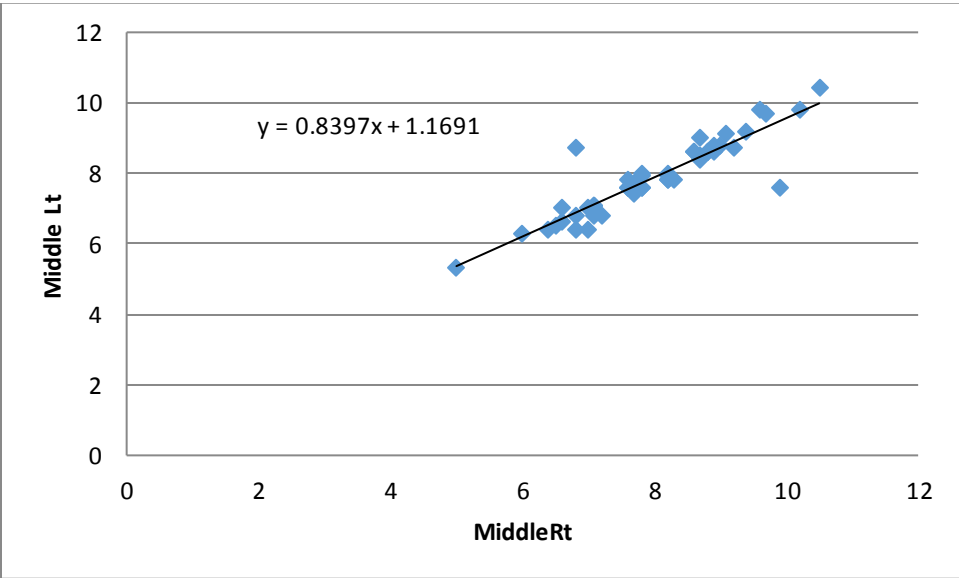


Figure 4.4 show correlation between lower right and lower left common femoral artery

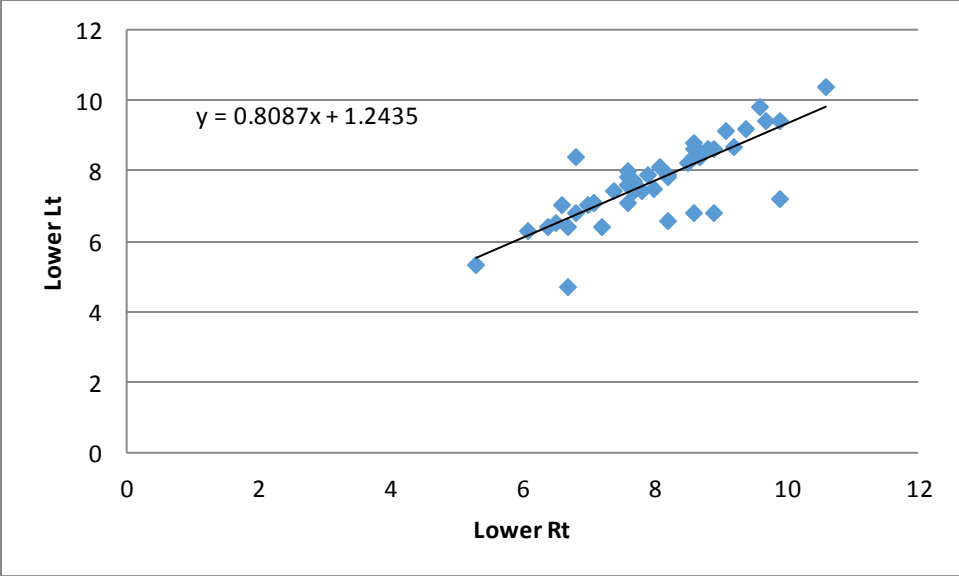


Figure 4.5 show correlation between bifurcation and upper right common femoral artery

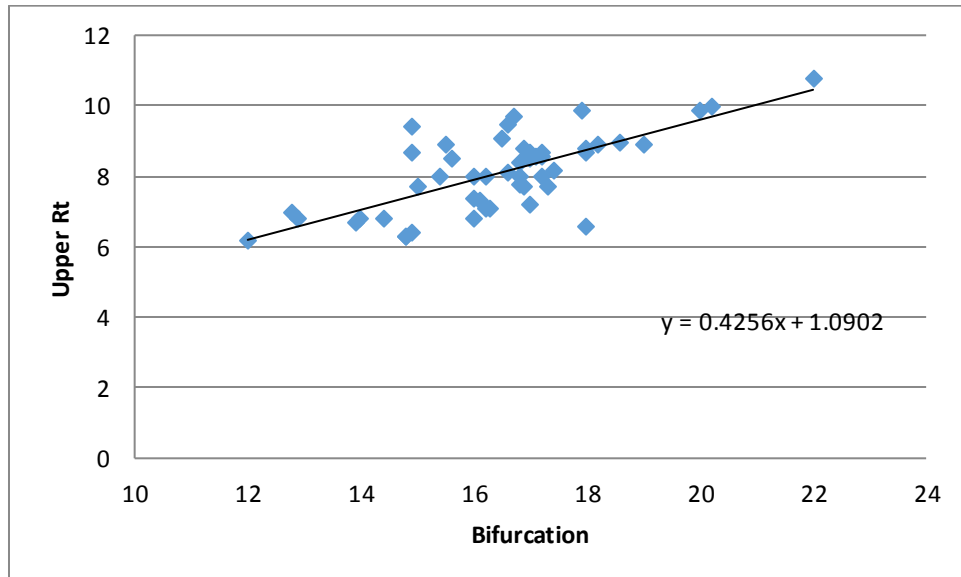


Figure 4.6 show correlation between bifurcation and upper left common femoral artery

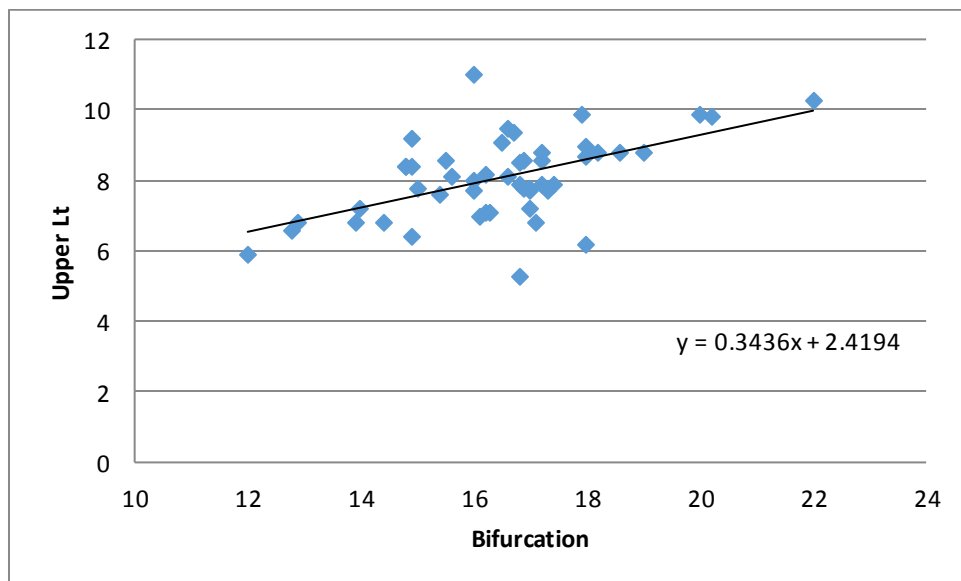


Figure 4.7 show correlation between bifurcation and middle right common femoral artery

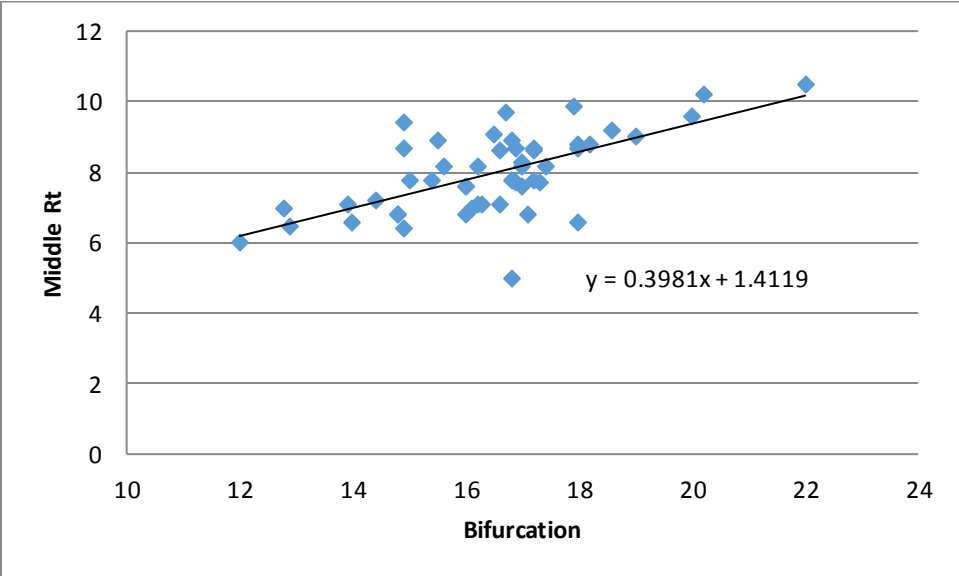


Figure 4.8 show correlation between bifurcation and middle left common femoral artery

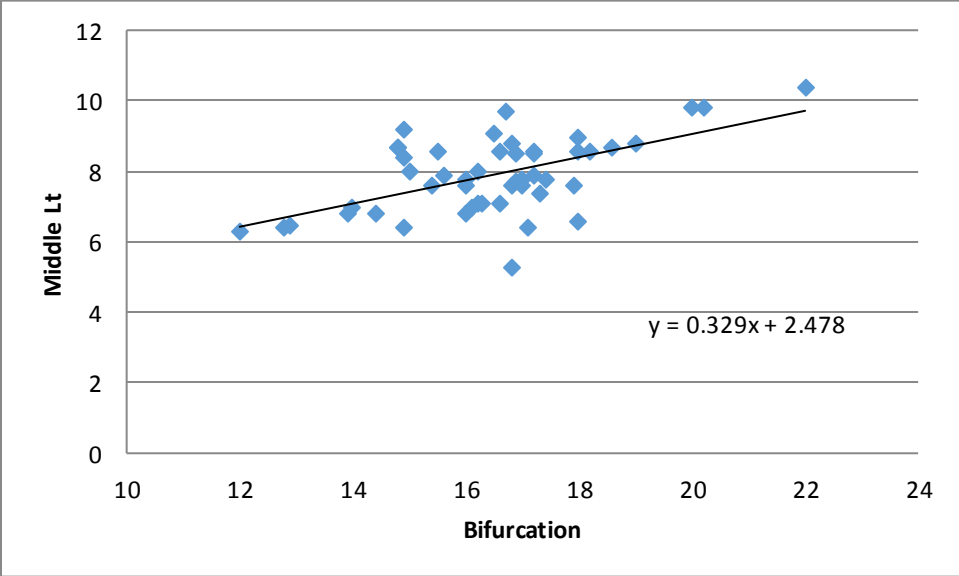


Figure 4.9 show correlation between bifurcation and lower right common femoral artery

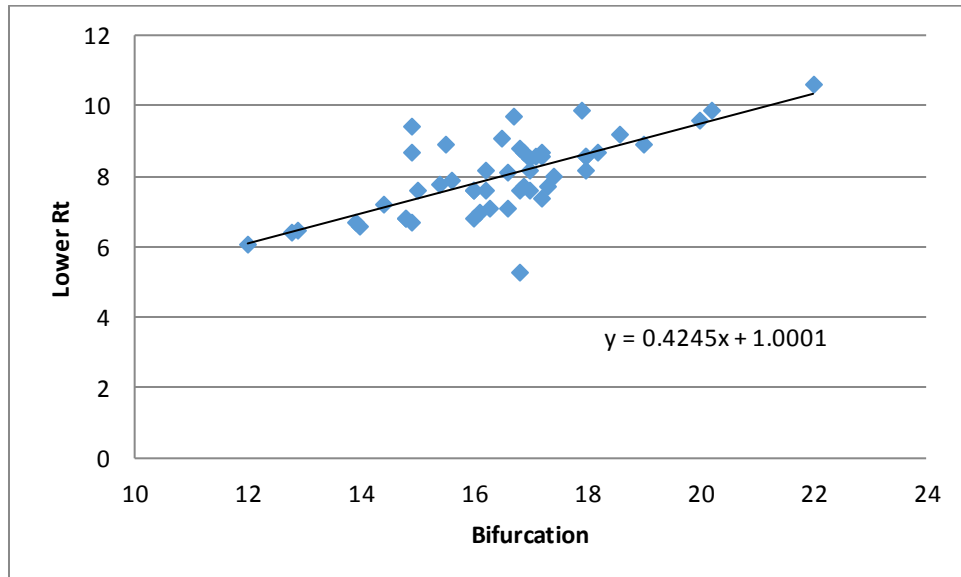


Figure 4.10 show correlation between bifurcation and lower left common femoral artery

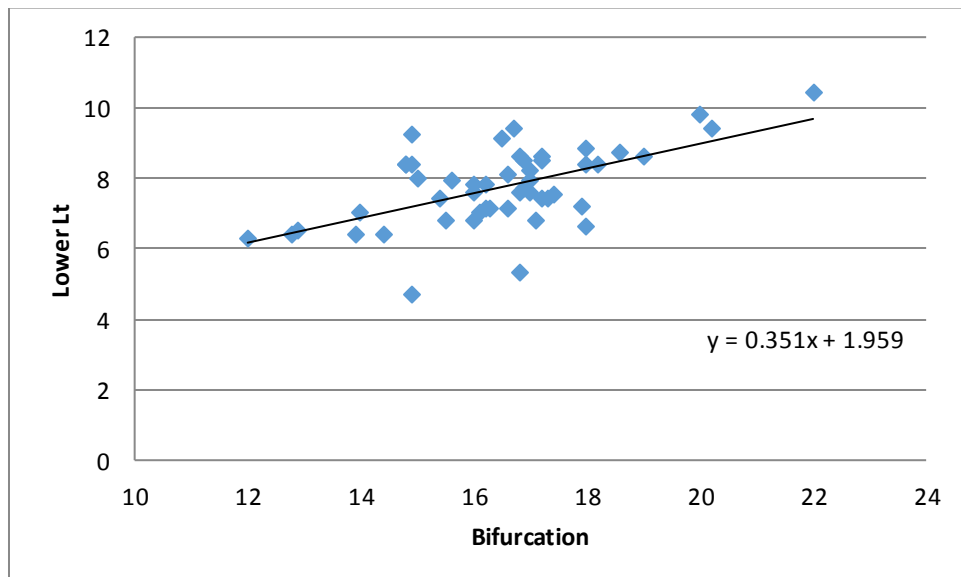


Table 4.7 show statistical description of normal and diabetics patients

| Classes | | Mean | Std. Deviation |
|-------------|----------|---------|----------------|
| lower_Lt | Normal | 7.740 | 1.1075 |
| | Diabetes | 5.128 | 2.3988 |
| medium_Lt | Normal | 7.896 | 1.0662 |
| | Diabetes | 5.750 | 2.1644 |
| upper_Lt | Normal | 8.078 | 1.1687 |
| | Diabetes | 6.894 | 1.6572 |
| lower_Rt | Normal | 7.992 | 1.1089 |
| | Diabetes | 5.322 | 1.8139 |
| medium_Rt | Normal | 7.9680 | 1.15819 |
| | Diabetes | 5.7926 | 1.52981 |
| upper_Rt | Normal | 8.100 | 1.1101 |
| | Diabetes | 6.561 | 1.3677 |
| Bifurcation | Normal | 16.4700 | 1.84759 |
| | Diabetes | 14.8993 | 2.86645 |

Table 4.8 show statistical description of normal and hypertensive patients

| Classes | | Mean | Std. Deviation |
|-------------|--------------|---------|----------------|
| lower_Lt | Normal | 7.740 | 1.1075 |
| | Hypertensive | 7.348 | 2.0344 |
| medium_Lt | Normal | 7.896 | 1.0662 |
| | Hypertensive | 7.554 | 1.5871 |
| upper_Lt | Normal | 8.078 | 1.1687 |
| | Hypertensive | 7.848 | 1.4733 |
| lower_Rt | Normal | 7.992 | 1.1089 |
| | Hypertensive | 6.566 | 2.1859 |
| medium_Rt | Normal | 7.9680 | 1.15819 |
| | Hypertensive | 7.3678 | 1.88747 |
| upper_Rt | Normal | 8.100 | 1.1101 |
| | Hypertensive | 7.764 | 1.8051 |
| Bifurcation | Normal | 16.4700 | 1.84759 |
| | Hypertensive | 17.1940 | 2.11597 |

Figure 4.11 compare means for bifurcation of abdominal aorta between normal, diabetic and hypertensive patients

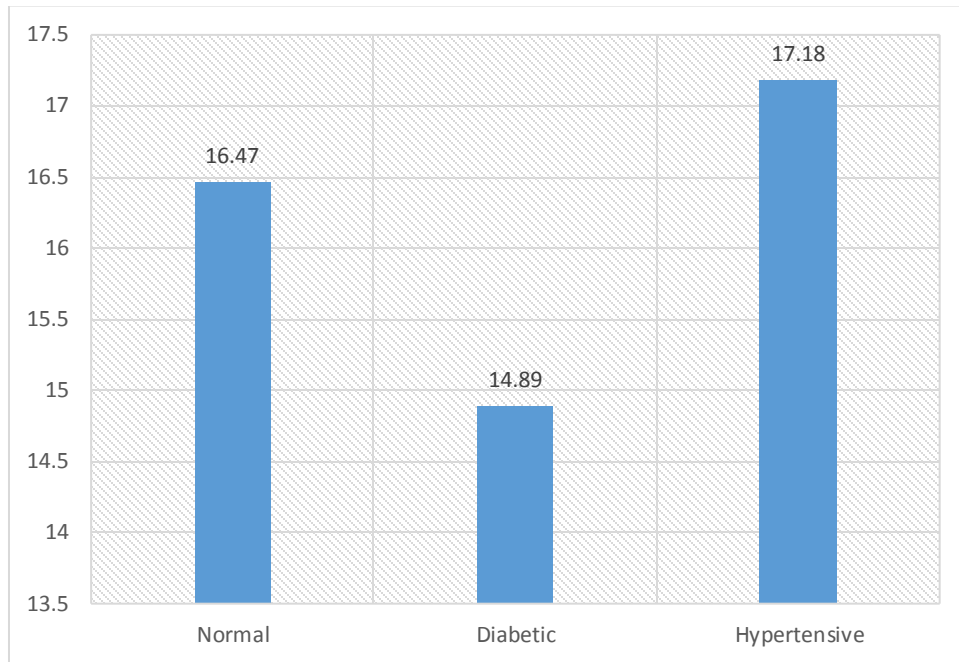


Figure 4.12 compare means for common femoral artery between normal, diabetic and hypertensive patients

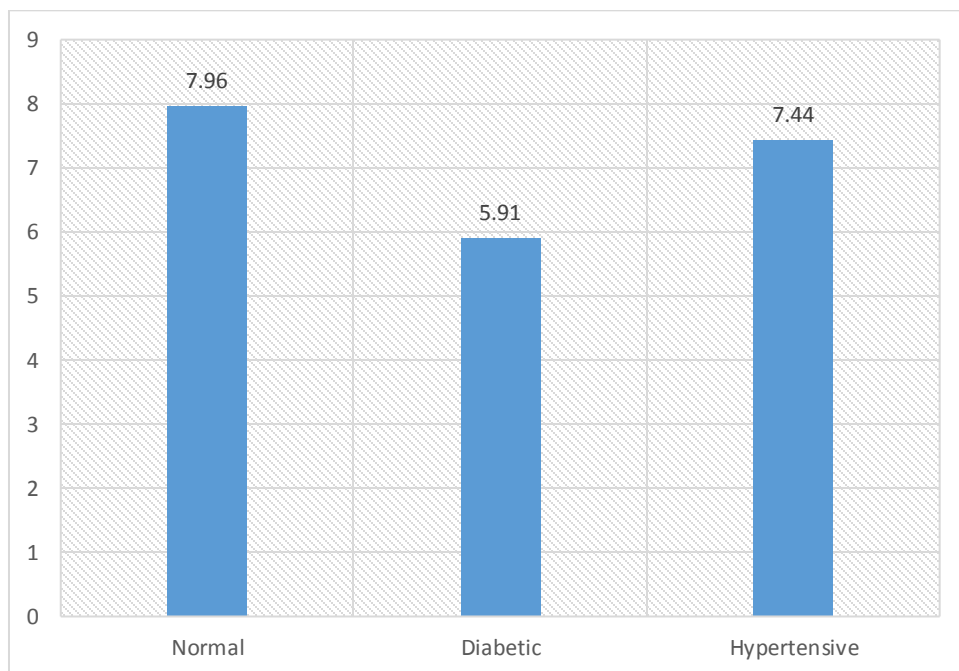


Table 4.9 show independent sample T-Test for equality of means for normal and diabetes patients

| Independent Samples Test normal & diabetes | | |
|--|------------------------------|-----------------|
| | t-test for Equality of Means | |
| | t | Sig. (2-tailed) |
| lower_Lt | 7.035 | .000 |
| medium_Lt | 6.334 | .000 |
| upper_Lt | 4.178 | .000 |
| lower_Rt | 8.969 | .000 |
| medium_Rt | 8.126 | .000 |
| upper_Rt | 6.270 | .000 |
| Bifurcation | 3.292 | .001 |

Table 4.10 show independent sample T-Test for equality of means for normal and hypertensive patients

| Independent Samples Test normal & hypertensive | | |
|--|------------------------------|-----------------|
| | t-test for Equality of Means | |
| | t | Sig. (2-tailed) |
| lower_Lt | 1.197 | .234 |
| medium_Lt | 1.265 | .209 |
| upper_Lt | .865 | .389 |
| lower_Rt | 4.114 | .000 |
| medium_Rt | 1.916 | .058 |
| upper_Rt | 1.121 | .265 |
| Bifurcation | -1.822 | .071 |

Fig 4.13 Show Error bar for normal, diabetics and hypertensive for left lower common femoral artery

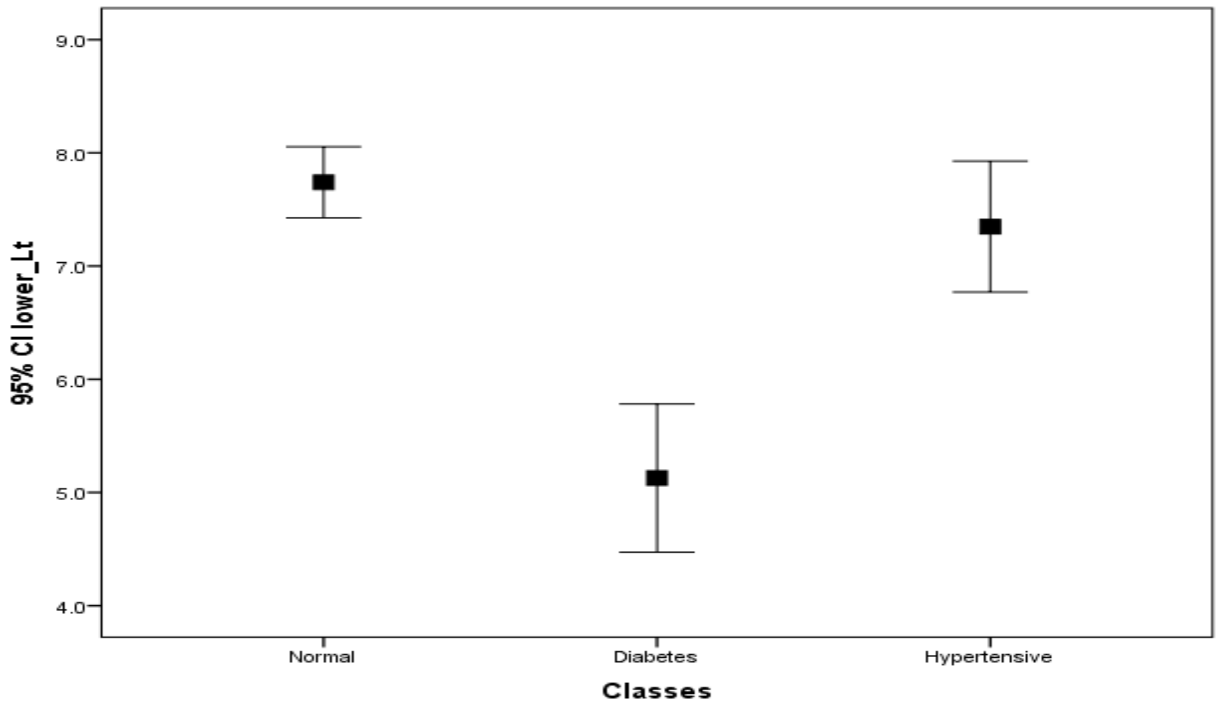


Fig 4.14 Show Error bar for normal, diabetics and hypertensive for right lower common femoral artery

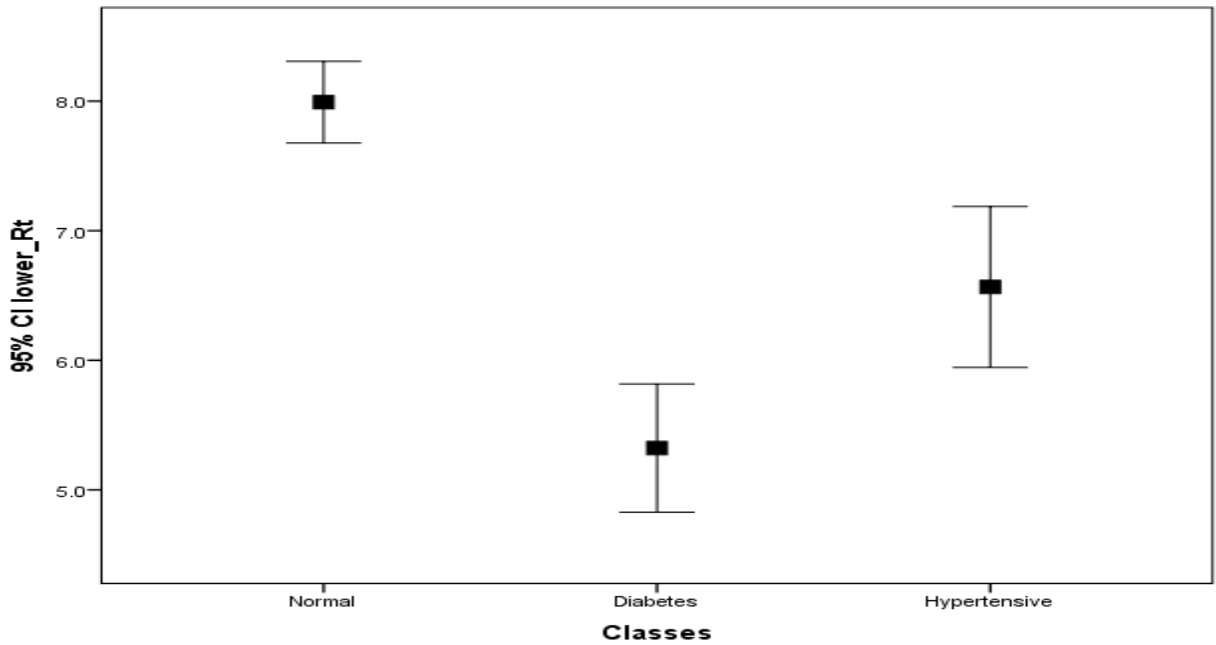


Fig 4.15 Show Error bar for normal, diabetics and hypertensive for left medium common femoral artery

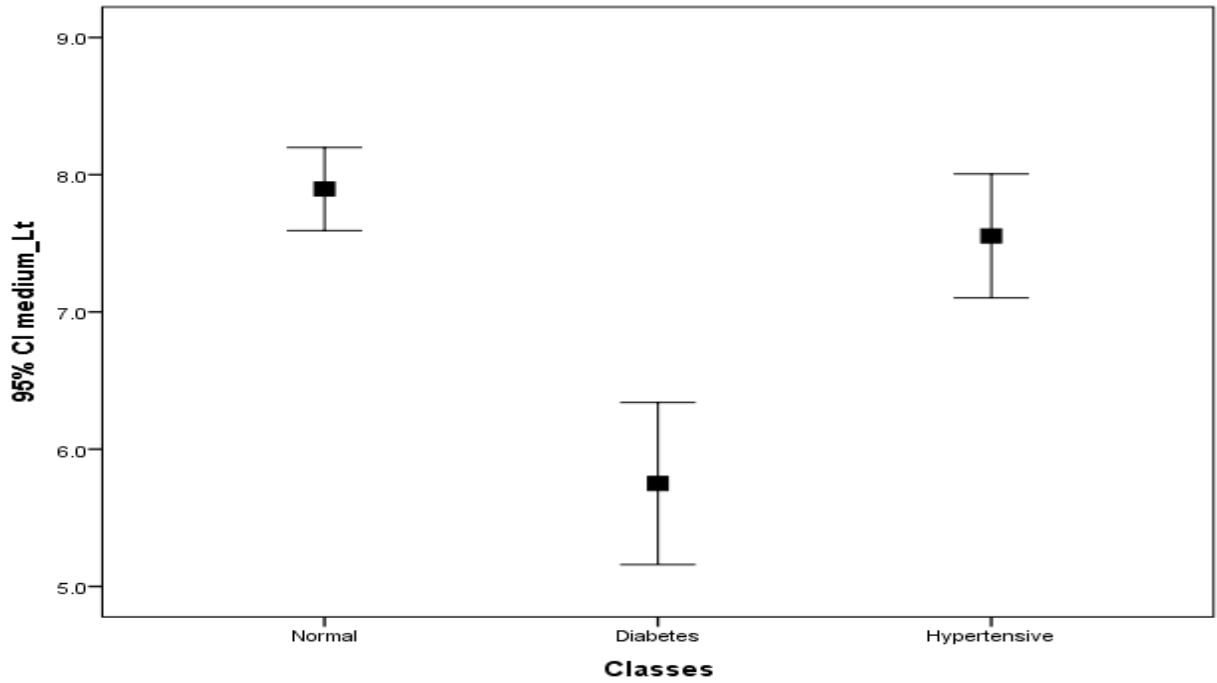


Fig 4.16 Show Error bar for normal, diabetics and hypertensive for right medium common femoral artery

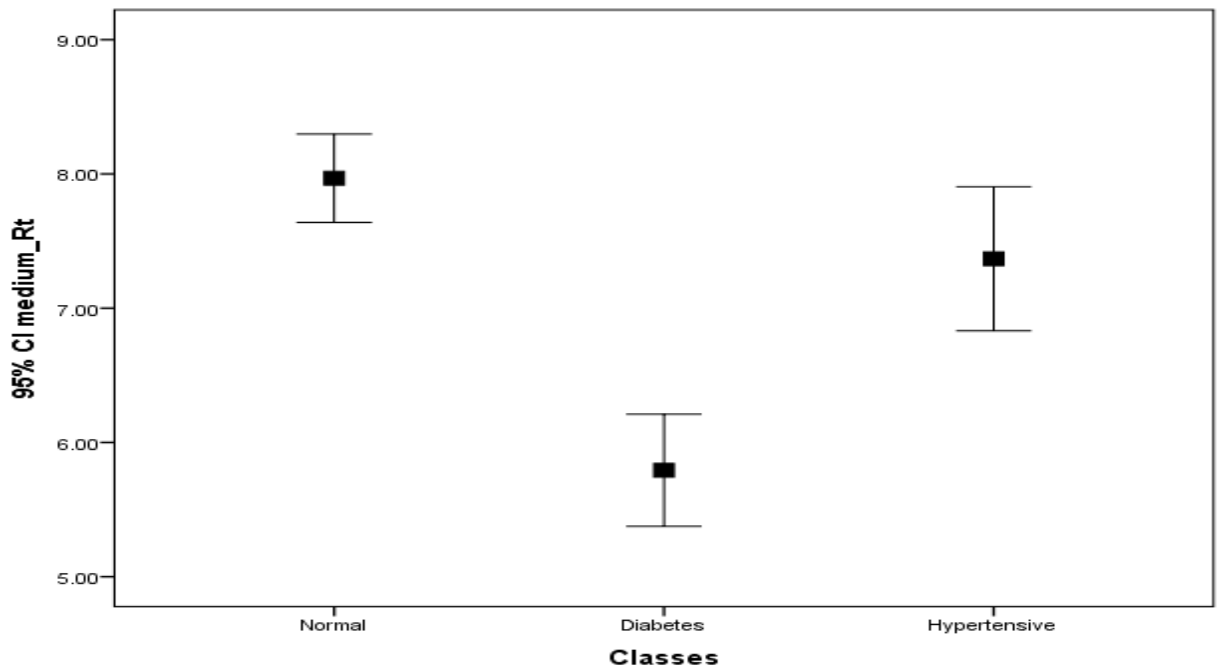


Fig 4.17 Show Error bar for normal, diabetics and hypertensive for left upper common femoral artery

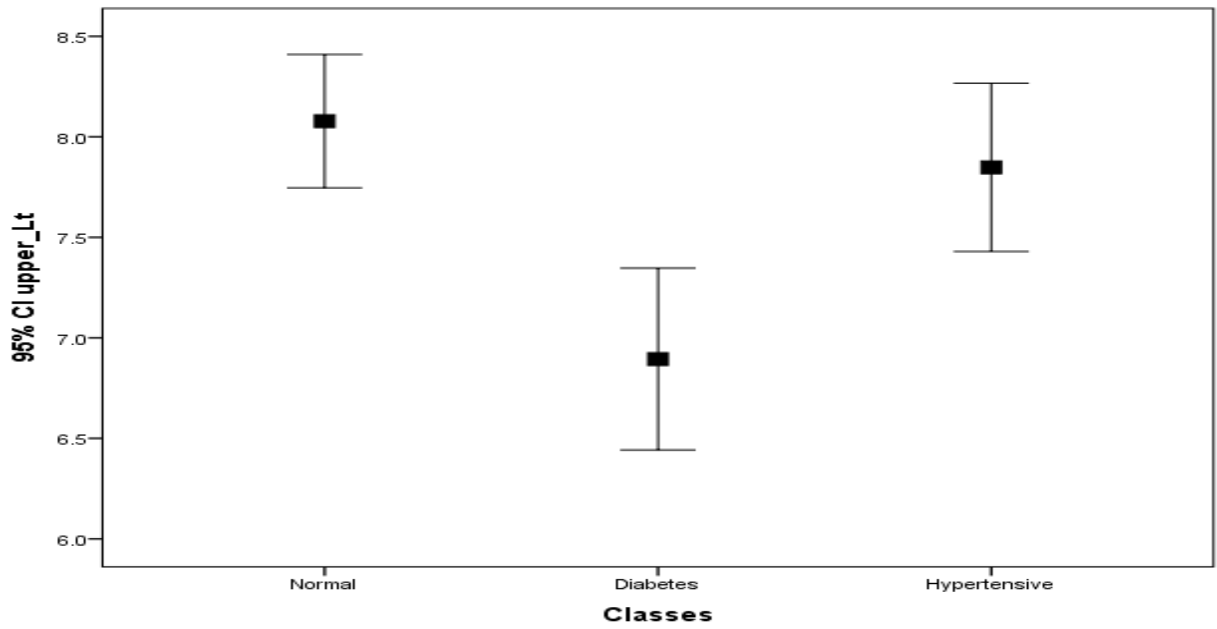


Fig 4.18 Show Error bar for normal, diabetics and hypertensive for right upper common femoral artery

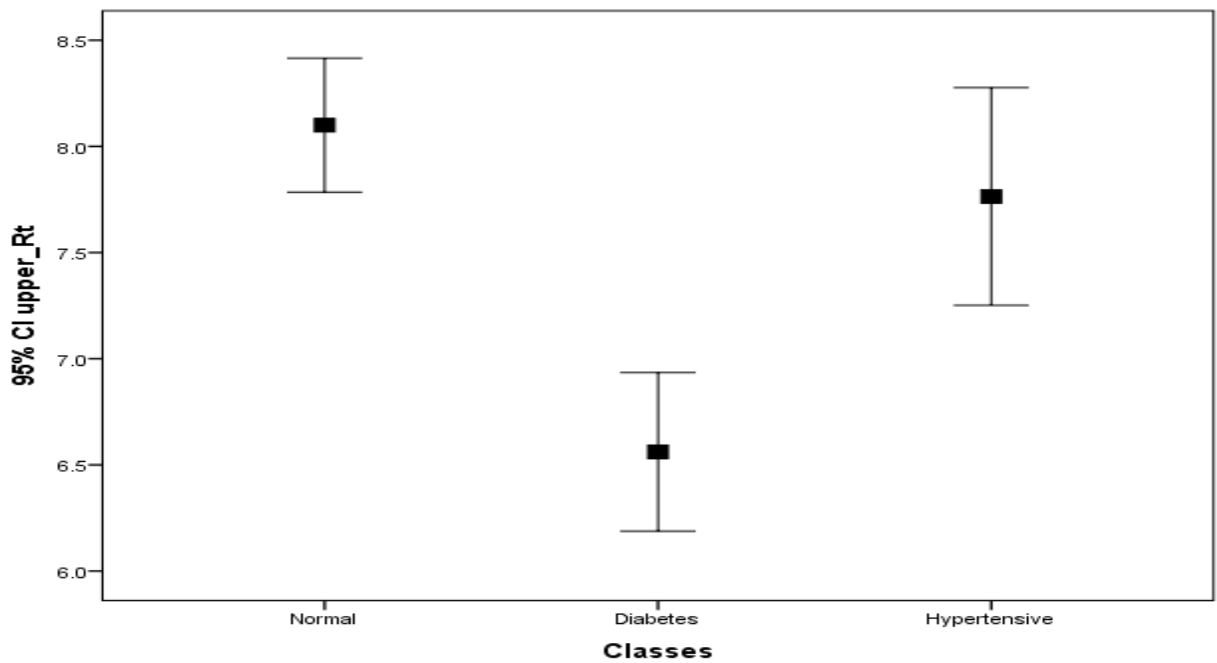
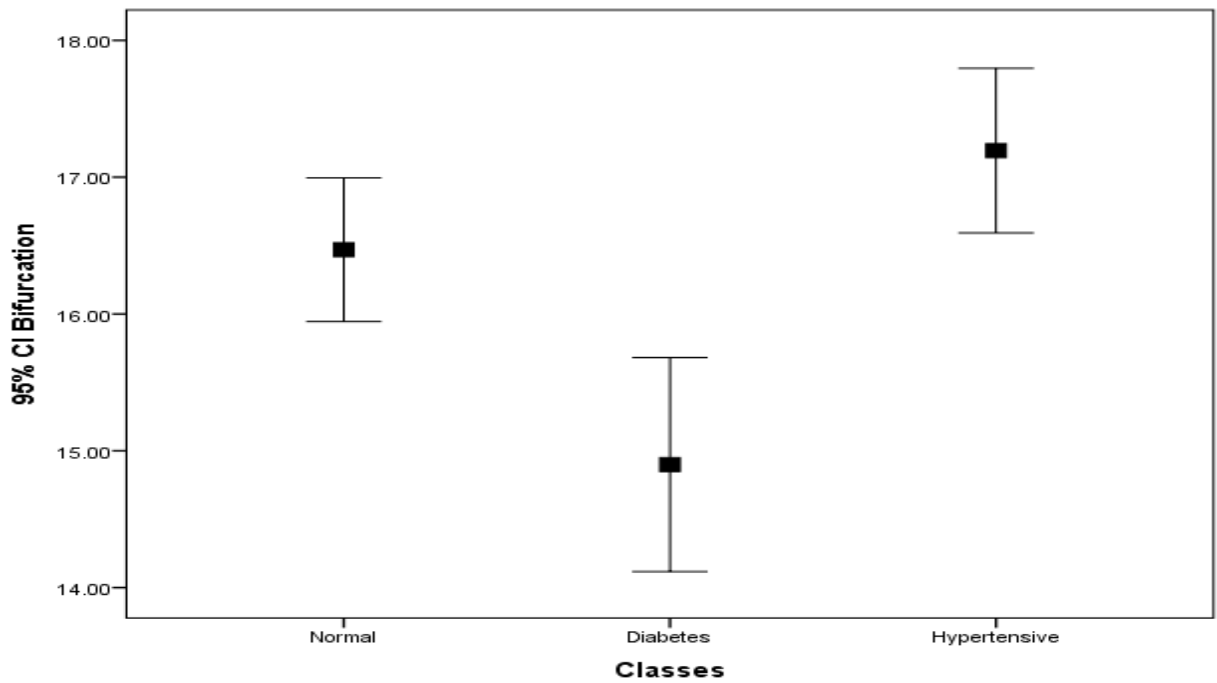


Fig 4.19 Show Error bar for normal, diabetics and hypertensive for bifurcation of abdominal artery



Chapter Five

5.1 Discussion:

Measurement of abdominal aorta at its bifurcation as well as left and right common femoral artery for 300 patients (100 normal, 100 diabetic and 100 hypertensive patients).

For the normal measurements reveals that, male has slightly wider diameter than female but this differences were insignificant at $p = 0.05$ using t-test, which means in normal patients gender has no effect on the diameter dimensions variability between the gender except for Rt upper common femoral part (Table 4.1 & 4.2).

The mean diameter of lower, medium and upper part of the Rt and Lt branch of the common femoral artery was 7.74 ± 1.11 , 7.99 ± 1.11 , 7.89 ± 1.07 , 7.96 ± 1.16 , 8.08 ± 1.17 and 8.10 ± 1.11 mm respectively (Table 3). These measurements showed similarity between the Rt and Lt common femoral artery in the three parts, but using t-test there is a significant differences between the lower common femoral part (Rt and Lt) as shown in (Table 4), but there is strong correlation between the Rt and Lt common femoral branches at the lower, medium and upper parts as shown in (Table 4.4).

The bifurcation showed inconclusive results regarding the gender; as well it has strong correlation with the Rt and left common femoral artery at it is three parts (lower, medium and upper). This means we can estimate the dimension of these parts using the dimension of the bifurcation. Linear regression results showed that the rate of change in the lower Lt and Rt common femoral artery

increases by 0.351mm(fig 4.1) and 0.4245mm (fig 4.2) respectively for each mm of bifurcation. For the medium Lt and Rt the rate of change was 0.329mm (fig 4.3) and 0.398mm (fig 4.4) for each one mm of bifurcation as well as for the upper common femoral part Lt and Rt it was 0.343mm (fig 4.5) and 0.425mm (fig 4.6) respectively for each mm of the bifurcation. All these parameters showed that there is a direct linear relationship between the common femoral parts (Rt and Lt) with the bifurcation, where the diameters for any part can be estimated positively if the diameter of the aorta at bifurcation were normal.

And when comparison between the normal and up normal patients (diabetic and hypertensive patients) the results was:

Measurement of the lower, medium and upper left common femoral artery (mean \pm SD) for normal was 7.74 \pm 1.11, 7.89 \pm 1.07 and 8.08 \pm 1.17mm respectively while for diabetic patients were 5.13 \pm 2.39, 5.75 \pm 2.16 and 6.89 \pm 1.66; this result showed that there is differences between the normal and diabetic patients concerning left common femoral artery. This differences was significant using t-test at $p = 0.05$ (Table 4.7&4.8). For the Rt side the measurement for normal patient it was 7.99 \pm 1.11, 7.96 \pm 1.16 and 10 \pm 1.11 mm respectively while for diabetic patient it was 5.32 \pm 1.81, 5.97 \pm 1.53 and 6.56 \pm 1.37 mm respectively also these differences was significant. These results dictated that in diabetic patient the diameter of the common femoral artery (Lt and Rt) at lower, medium and upper part were smaller than the normal patient. Similarly the diameter at bifurcation showed significant differences between the normal and diabetic patients where the

diameter was larger in normal than diabetic; 16.47 ± 1.85 and 14.89 ± 2.87 mm for normal and diabetic respectively (Table 4.7).

The measurement for hypertensive patients in respect to the previous normal values was as follows; for Lt Side of the common femoral artery were 7.35 ± 2.03 , 7.55 ± 1.59 and 7.84 ± 1.47 mm this results showed slight change from the normal but this changes were not significant at $p = 0.05$ using t-test. While for the Rt side the measurement was 6.57 ± 2.18 , 7.36 ± 1.88 and 7.78 ± 1.81 mm only the lower Rt part of the common femoral artery showed significant difference from normal; where the diameter in normal was larger than the that of hypertensive patient. Concerning bifurcation there is difference between the normal and hypertensive patient; where it is slightly larger in hypertensive than normal 17.19 ± 2.12 and 16.47 ± 1.85 but this differences were inconclusive using t-test at $p = 0.05$.

Figure 2, 3, 4, 5, 6, 7 and 8 an Error bar showed the distribution of the average diameter for the left and right side of common femoral artery and abdominal aorta bifurcation.

5.2 Conclusion:

The diameter of the abdominal aorta at its bifurcation to left and right common femoral artery, for the normal measurements there is slightly increases with gender its larger at male than female but this was inconclusive. The common femoral artery Rt and left branches at lower, medium and upper can be estimated using the following linear equations:

Equation for the regression values between the bifurcation and the:

$$\text{Lower left common femoral artery} = (0.35 \times \text{bifurcation}) + 1.96$$

$$\text{Lower right common femoral artery} = (0.42 \times \text{bifurcation}) + 1.00$$

$$\text{Medium left common femoral artery} = (0.33 \times \text{bifurcation}) + 2.48$$

$$\text{Medium right common femoral artery} = (0.39 \times \text{bifurcation}) + 1.41$$

$$\text{Upper left common femoral artery} = (0.34 \times \text{bifurcation}) + 2.42$$

$$\text{Upper right common femoral artery} = (0.43 \times \text{bifurcation}) + 1.09$$

When compare between the normal with diabetic and hypertensive patients, the diameter of left and right common femoral artery, the diameter of normal larger than the diameter of hypertensive and diabetic patients, but significant in case of diabetic patients, for abdominal aorta bifurcation the hypertensive patients showed slightly larger diameter than normal and diabetic patient's diameter was smaller but this differences were inconclusive.

5.3 Recommendation:

- Existing technique can be applied for body vessels measurements.
- More studies can be done according to age and Body Mass Index (BMI).
- Include more diseases of peripheral arteries ; abdominal aorta and common femoral artery disease.
- Existing study using other modalities MRI and Ultrasound.

References

Beregi JP, Elkohen M, Deklunder G, et al. Helical CT angiography compared with arteriography in the detection of renal artery stenosis. *AJR Am J Roentgenol* 1996; 167:495–501.

Beregi JP., Djabbari M., Desmoucelle F.: Popliteal vascular disease: Evaluation with spiral CT Angiography. *Radiology* 1997; 203; 477-483.

Brewster DC.: Prosthetic grafts. In: Veith FJ, et al, eds. *Vascular surgery: principles and practice*. 2nd ed. New York, NY: McGraw-Hill, 1994; 559-583.

Catalano C, Fraioli F, Laghi A, et al: Infrarenal aortic and lower-extremity arterial disease: diagnostic performance of multi-detector row CT angiography. *Radiology* 231: 555-63, 2004.

Criqui MH, Fronek A, Barrett O et al. The prevalence of peripheral vascular arterial disease in a defined population. *Circulation* 1985; 71: 510-515.

Davies R, Neiman H, Yao J, Bergan J. Ultrasound scan diagnosis of peripheral aneurysms. *Arch Surg* 1977; 112: 55-8.

Dawson I., Brand R.: Popliteal artery aneurysm: long term follow-up of aneurysmal disease and results of surgical treatment. *J Vasc Surgery* 1991; 13; 398-407.

Graham LM.: Common femoral and popliteal aneurysm. In Rutherford RB, ed. *Vascular surgery*. 5th ed. Philadelphia, PA: Saunders 2000; 1345-1368.

Hansen F, Bergqvist D, Mangell P, Rydén Å, Sonesson B, Länne T. Non-invasive measurement of pulsatile vessel diameter change and elastic properties in human arteries: a methodological study. *Clin Physiol* 1993; 13: 631-43.

Henry Gray, *Anatomy of the Human Body*, Press Advertising 2001 Bartleby.com Van De Graaff: *Human Anatomy, Sixth Edition* © The McGraw-Hill Companies, 2001.

Hokanson E, Mozersky D, Sumner D, Strandness E. A phase-locked echo-tracking system for recording arterial diameter changes in vivo. *J Appl Physiol* 1972;32:728-33.

Iezzi R, Cotroneo AR, Pascali D et al. Multi-slice CT (MSCT) angiography for assessment of traumatic lesions of lower limb peripheral arteries. *Emerg Radiol.* 2007; 14: 389-94.

John E. Hall, Arthur C. Guyton, Guyton and Hall Textbook of Medical Physiology 2006, Elsevier Inc. 1600 John F. Kennedy Blvd., Suite 1800 Philadelphia, Pennsylvania 19103-2899.

Johnstone Kw, Rutherford Rb, Tilson Md, Shai~ Dm, Hollier L, Stanley JC. Suggested standards for reporting on arterial aneurysms. *J Vasc Surg* 1991; 13: 444-450.

Kanaoka Y, Ohci S, Mol-I T. Age-related changes in the abdominal aortic diameter. *Vasc Surg* 1994; 28: 349-358.

Kawasaki T, Sasayama S, Yagi SI, Asakawa T, Hirai T. Noninvasive assessment of the age related changes in stiffness of major branches of the human arteries. *Cardiovasc Res* 1987;21:678-87.

Kramer SC, Gorich J, Aschoff AJ, et al. Diagnostic value of spiral-CT angiography in comparison with digital subtraction angiography before and after peripheral vascular intervention. *Angiology* 1998; 49:599-606.

Länne T, Sandgren T, Mangell P, Sonesson B, Hansen F. Improved reliability of surveillance of abdominal aortic aneurysms. *Eur J Vasc Endovasc Surg* 1996;13:149-53.

Levi N, Schroeder TV. Arteriosclerotic common femoral artery aneurysms. *J Cardiovasc Surg* 1997;38:335.

Lewis P, Psaila JV, Davies WT, McCarty K, Woodcock JP. Measurement of volume flow in the human common femoral artery using a duplex ultrasound system. *Ultrasound Med Biol* 1986;12:777-84.

Li Ming X., Li Yu-hua: Evaluation of peripheral artery stent with 64-slice row CT angiography: prospective comparison with digital subtraction angiography. *European Journal of Radiology* 2009. Apr 17. [Epub ahead of print].

Lindstrom K, Gennser G, Sindberg Eriksen P, Benthin M, Dahl P. An improved echo-tracker for studies on pulse waves in the fetal aorta. In: Rolfe P, ed. *Fetal Physiological Measurements*. London: Butterworths, 1987: 217-226.

Lindström K, Gennser G, Sindberg Eriksen P, Benthin M, Dahl P. An improved echo-tracker for studies on pulse waves in the fetal aorta. In: Rolfe P, editor. *Fetal physiological measurements*. London: Butterworths; 1987. p. 217-26.

Lopera J., Trimmer C. K., Josephs S. G, Anderson M. E., Schuber S., Li R., Dolmatch B., Toursarkissian B.,: Multidetector CT Angiography of Infrainguinal Arterial Bypass. *RadioGraphics* 2008; 28:529-549.

Martin ML, Tay KH, Flak B: Multidetector CT angiography of the aortoiliac system and lower extremities: a prospective comparison with digital subtraction angiography. *AJR Am J Roentgenol* 180: 1085-91, 2003.

Moiler D, Cole Cw, Hill Gb. Epidemiology of abdominal aortic aneurysms: the effect of differing definitions. *Eur J Vasc Surg* 1992; 6: 647-650.

Ota H, Takase K, Igarashi K et al: MDCT compared with digital subtraction angiography for assessment of lower extremity arterial occlusive disease: importance of reviewing cross-sectional images. *AJR Am J Roentgenol* 182:201-9, 2004.

Pearce WH, Slaughter MS, Maise S, Salyapongse AN, Feinglass J, McCarthy WJ, et al. Aortic diameter as a function of age, gender and body surface area. *Surgery* 1993;114:691-5.

R. Iezzi, F. Pirro, M. Nestola, A. Simeone, L. Bonomo; Rome, Multi-detector row CT angiographic imaging of lower extremity vascular disease: A pictorial review of A, Nitecki SS, Linn S, et al. Multidetector CT angiography of peripheral vascular disease: a prospective comparison with intraarterial digital subtraction angiography. *AJR* 2003; 180:719-724.

Rieker O, Duber C, Schmiedt W, et al. Prospective comparison of CT angiography of the legs with intraarterial digital subtraction angiography. *AJR Am J Roentgenol* 1996; 166:269-276.

Rubin GD, Schmidt AJ, Logan LJ, et al. Multidetector-row CT angiography of lower extremity occlusive disease: a new application for CT scanning. *Radiology* 1999; 210:588.

Sandgren T, Sonesson B, Ahlgren ÅR, Länne T. Factors predicting the diameter of the popliteal artery in healthy humans. *J Vasc Surg* 1998;28:284-9.

Sonesson B, Länne T, Hansen F, Sandgren T. Infra-renal aortic diameter in the healthy person. *Eur J Vasc Surg* 1994; 8: 89-95.

Sonesson B, Länne T, Hansen F, Sandgren T. Infra-renal aortic diameter in the healthy person. *Eur J Vasc Surg* 1994;8:89-95.

Soto JA, Munera F, Morales C, et al. Focal arterial injuries of the proximal extremities: helical CT arteriography as the initial method of diagnosis. *Radiology* 2001; 218:188-194.

Sun Z.: Diagnostic accuracy of multislice CT angiography in peripheral arterial disease. *J Vasc Interv Radiol* 2006;17(12):1915-1921.

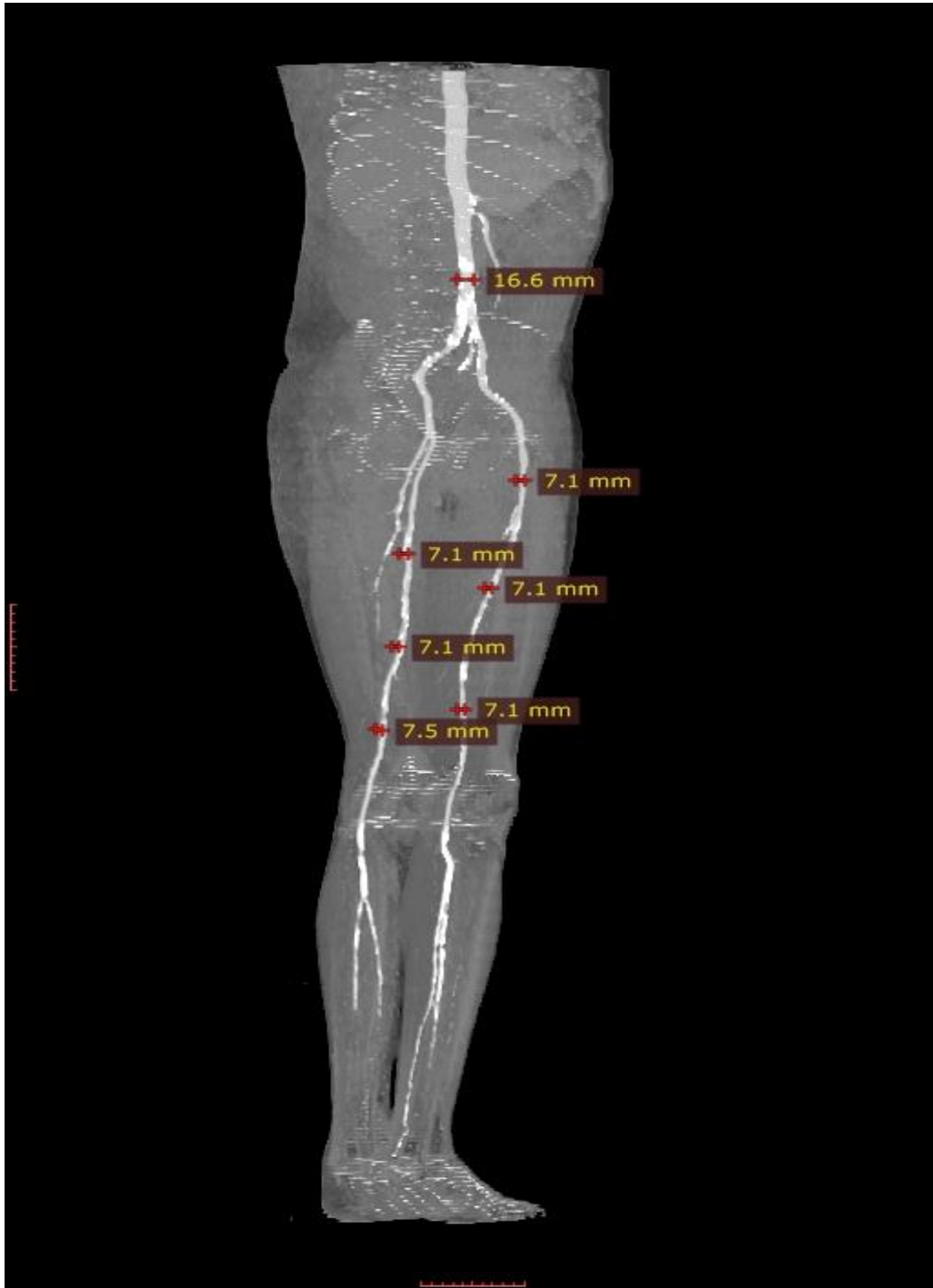
Thomas D. Boyer, Teresa L. Wright and Michael P. Manns, Zakim and Boyers Hepatology, Textbook of liver disease, fifth edition 2006.

Weiner SD, Reis ED, Kerstein MD. Peripheral arterial disease. Medical management in primary care practice. *Geriatrics* 2001 Apr; 56 (4): 20-2; 25-6; 29-30.

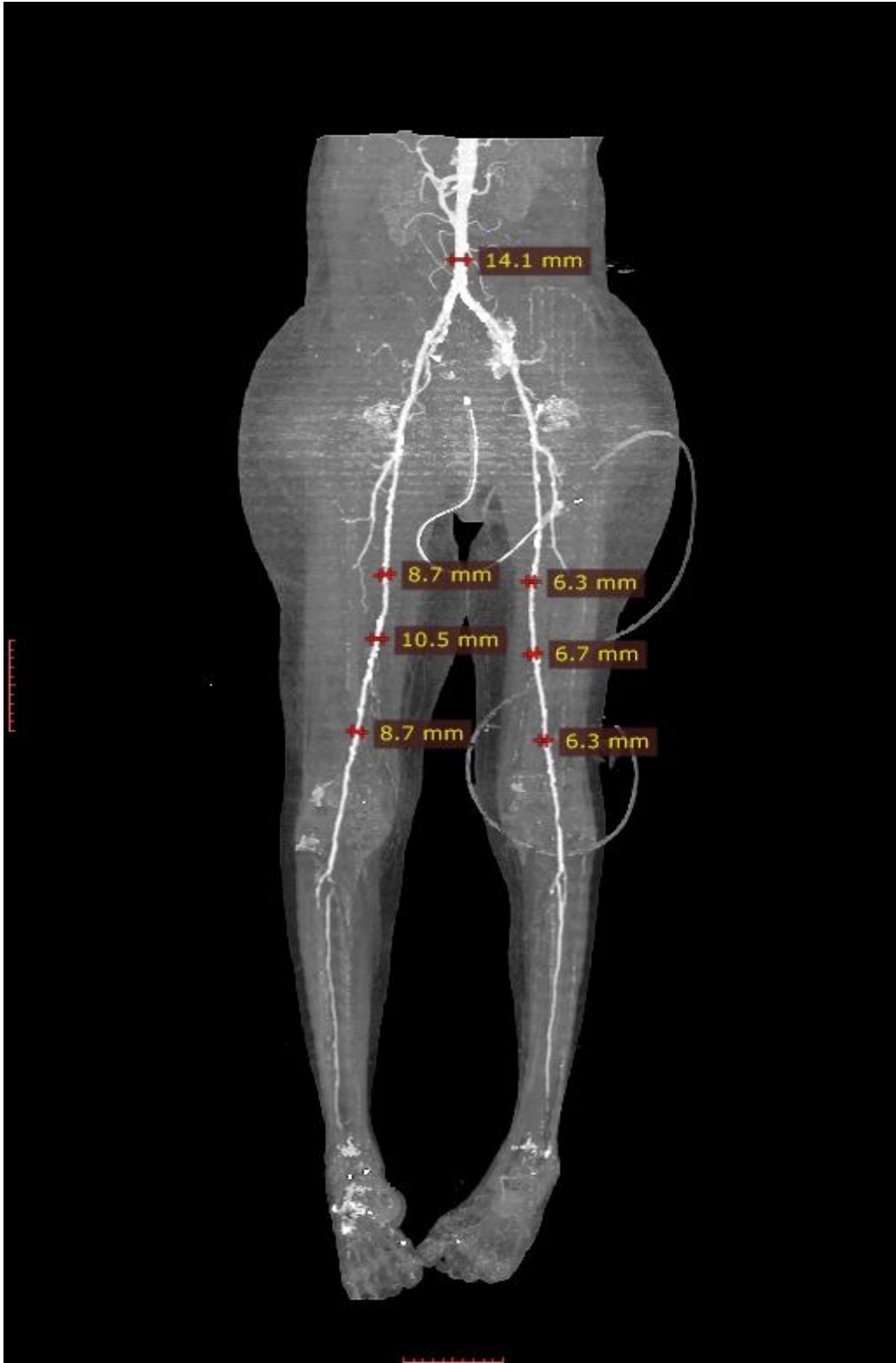
k/Willmann JK, Baumert B, Schertler T et al: Aortoiliac and lower extremity arteries assessed with 16-detector row CT angiography: prospective comparison with digital subtraction angiography. *Radiology* 236: 1083-93,2005.

Wright L. B., Matchett W., Cruz C. P., James C.: Popliteal artery disease: diagnosis and treatment. *Radiographics* 2004;24; 467-479.

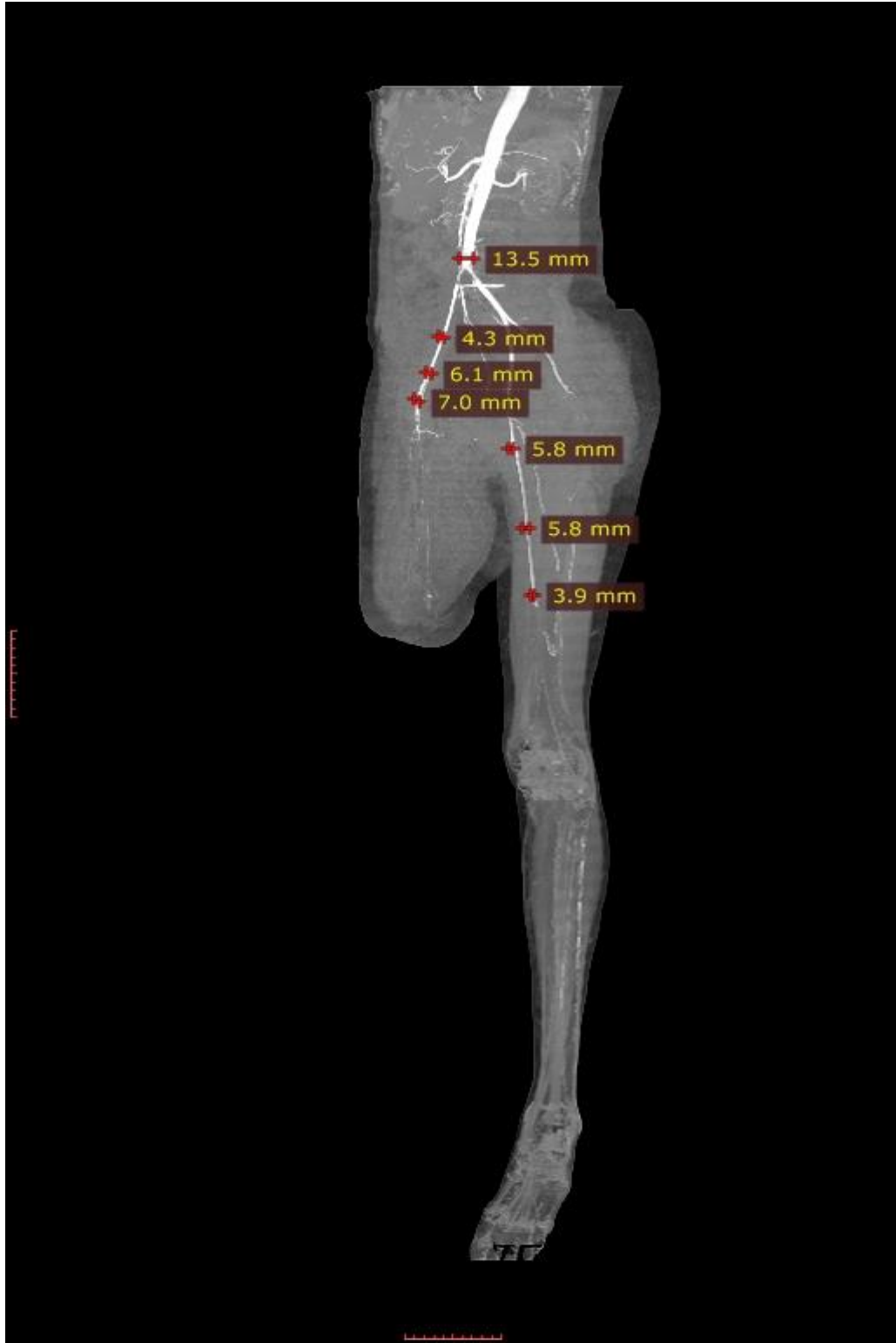
Appendices



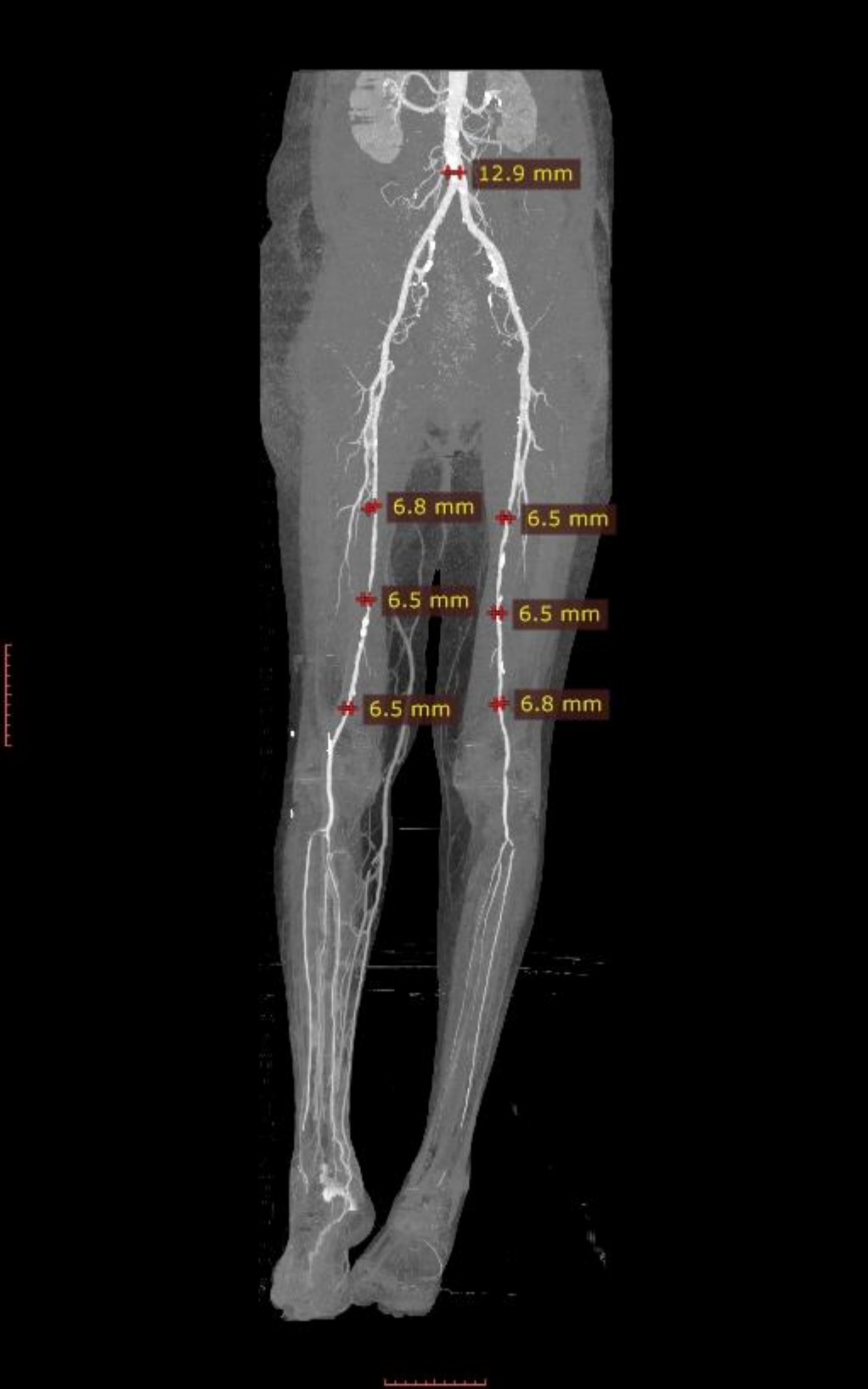
male normal

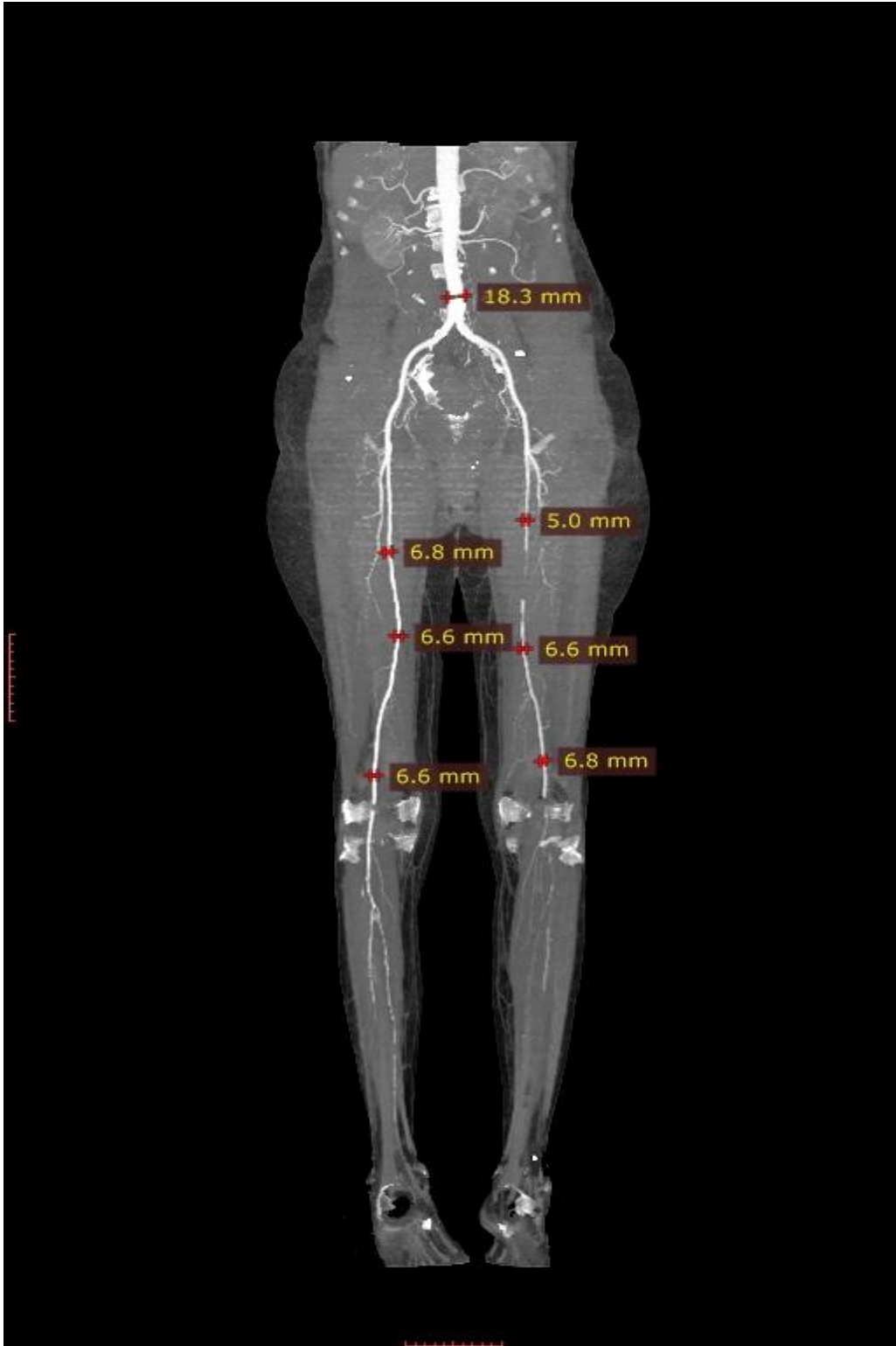


Normal female

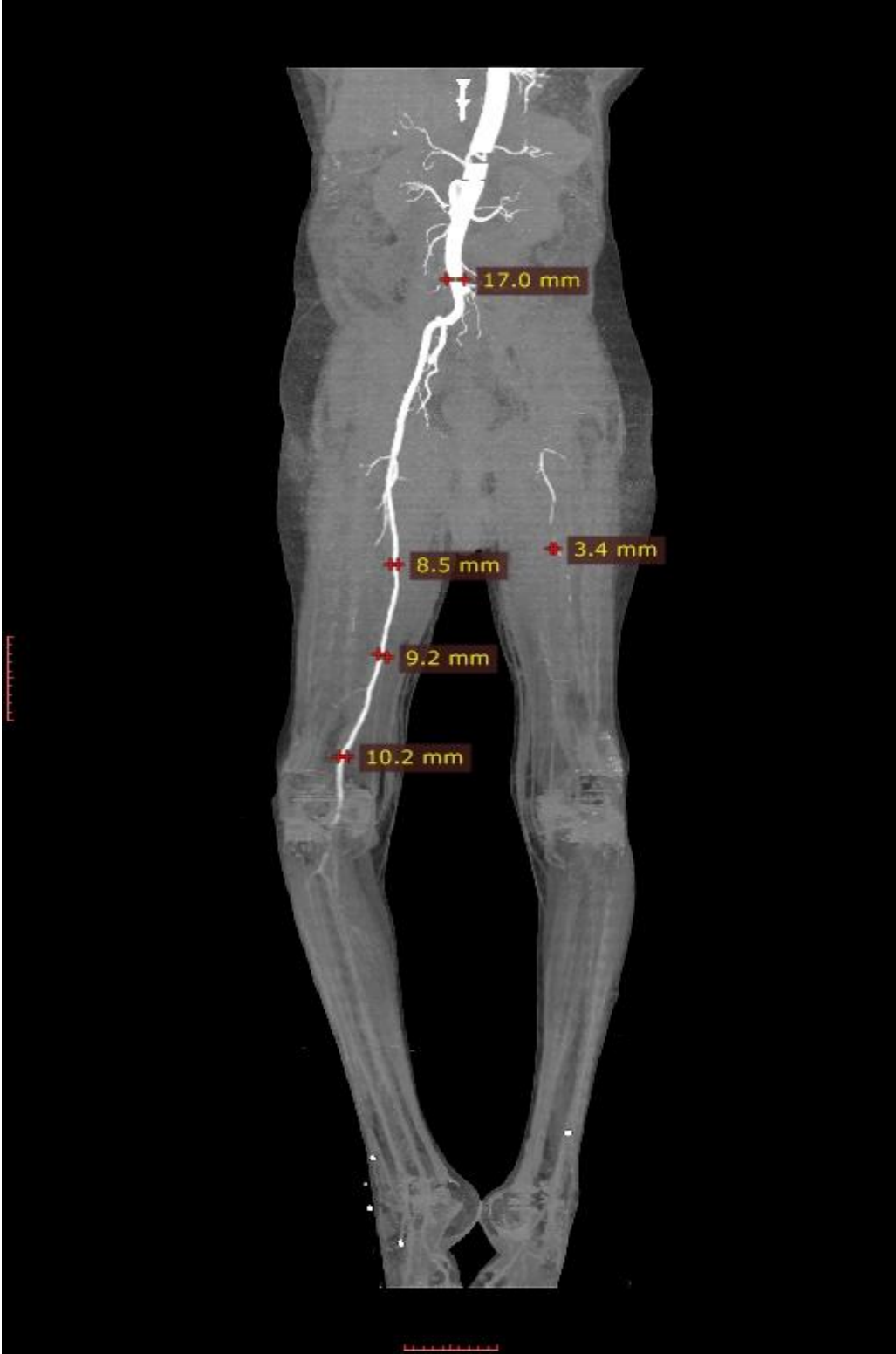


male diabetic

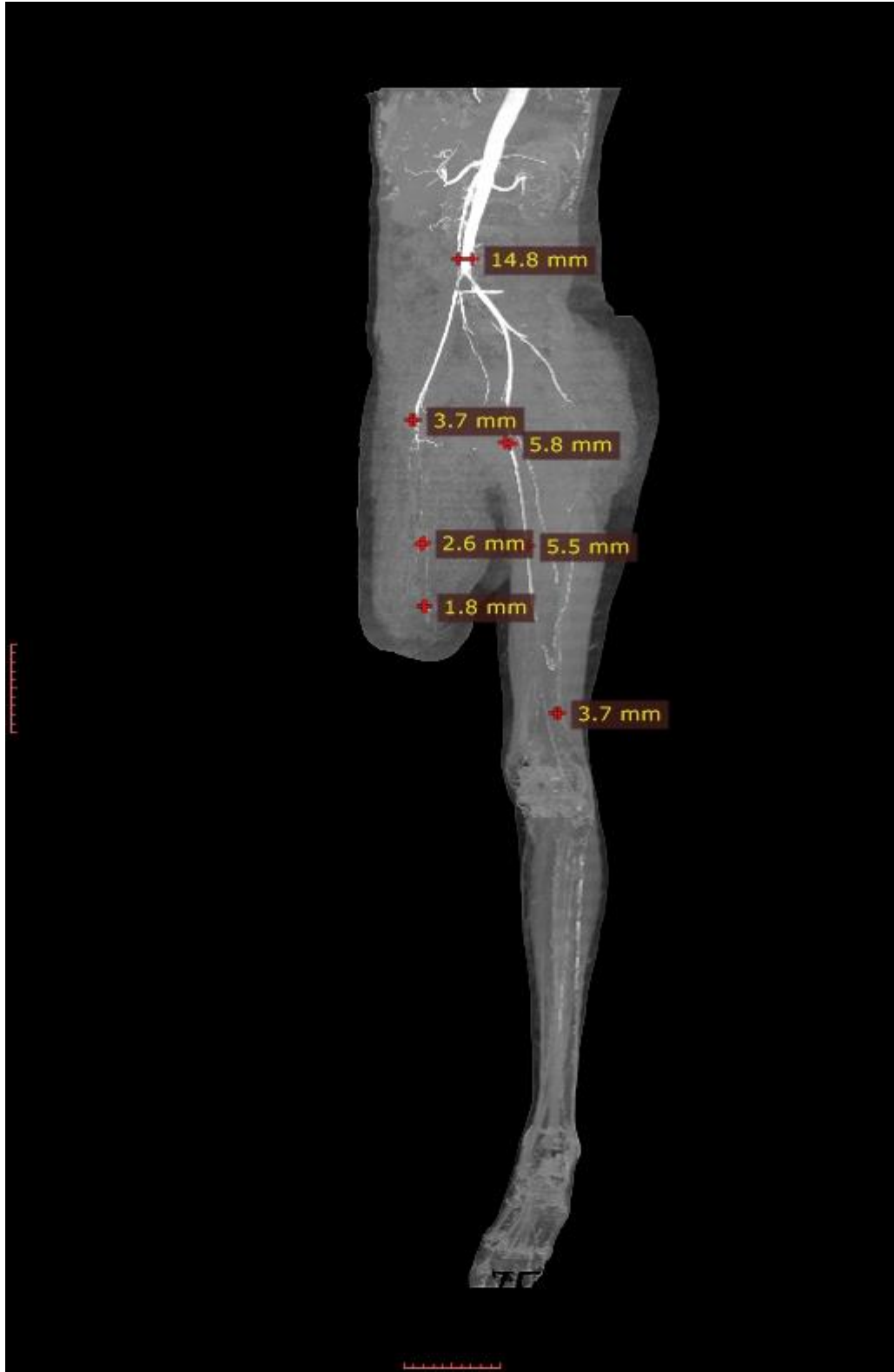




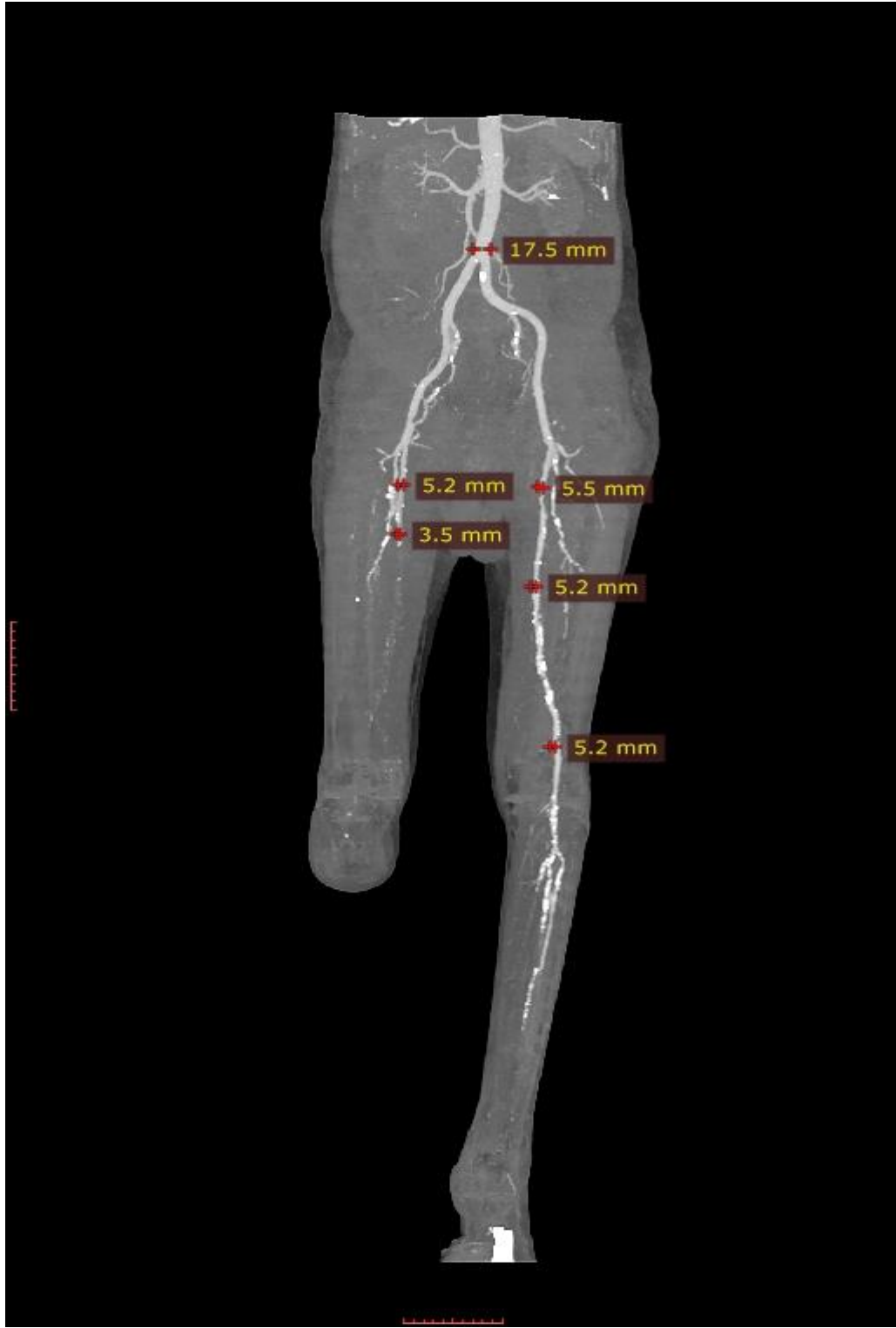
Normal Female



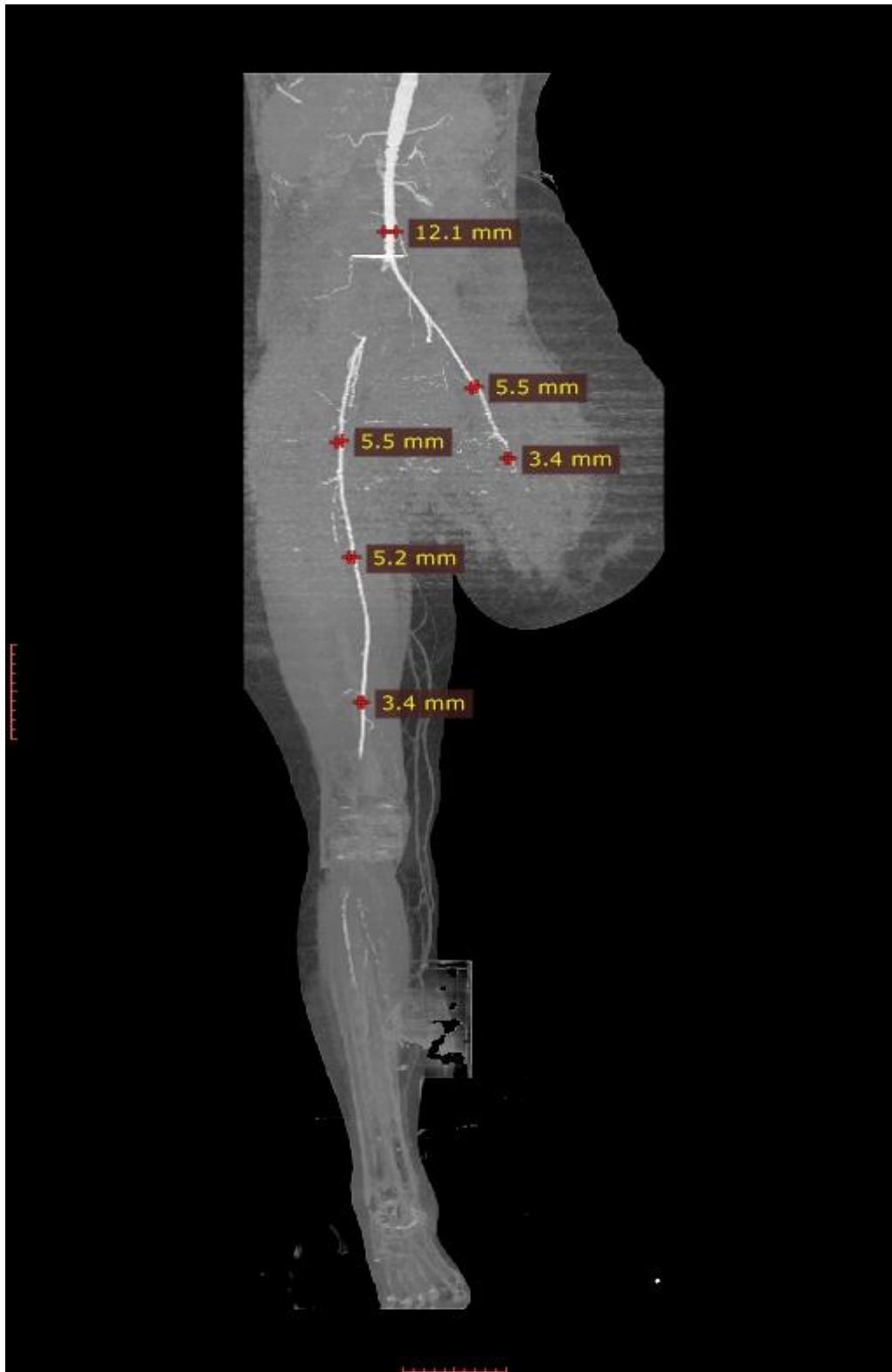
Male Diabetic



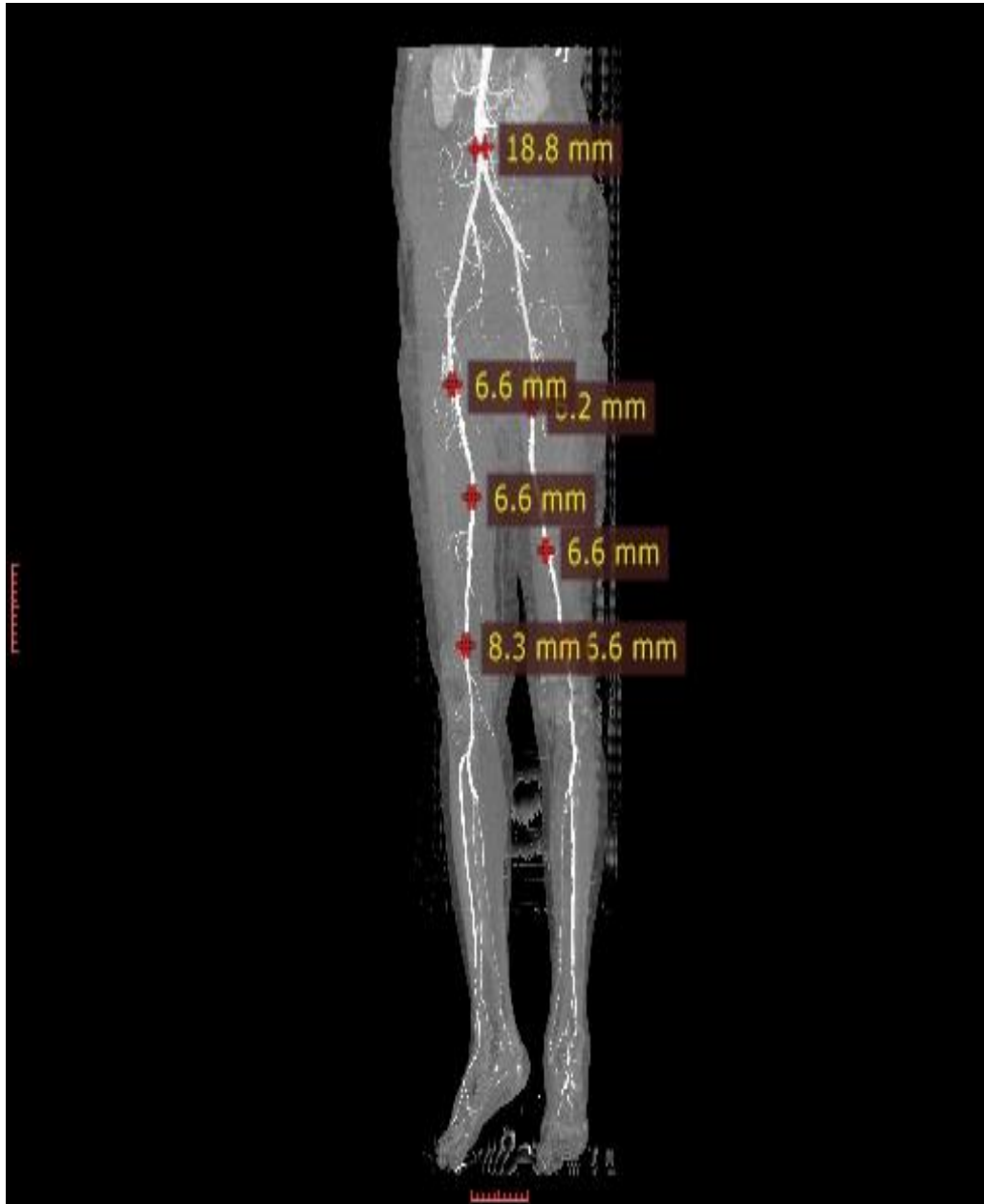
male diabetic



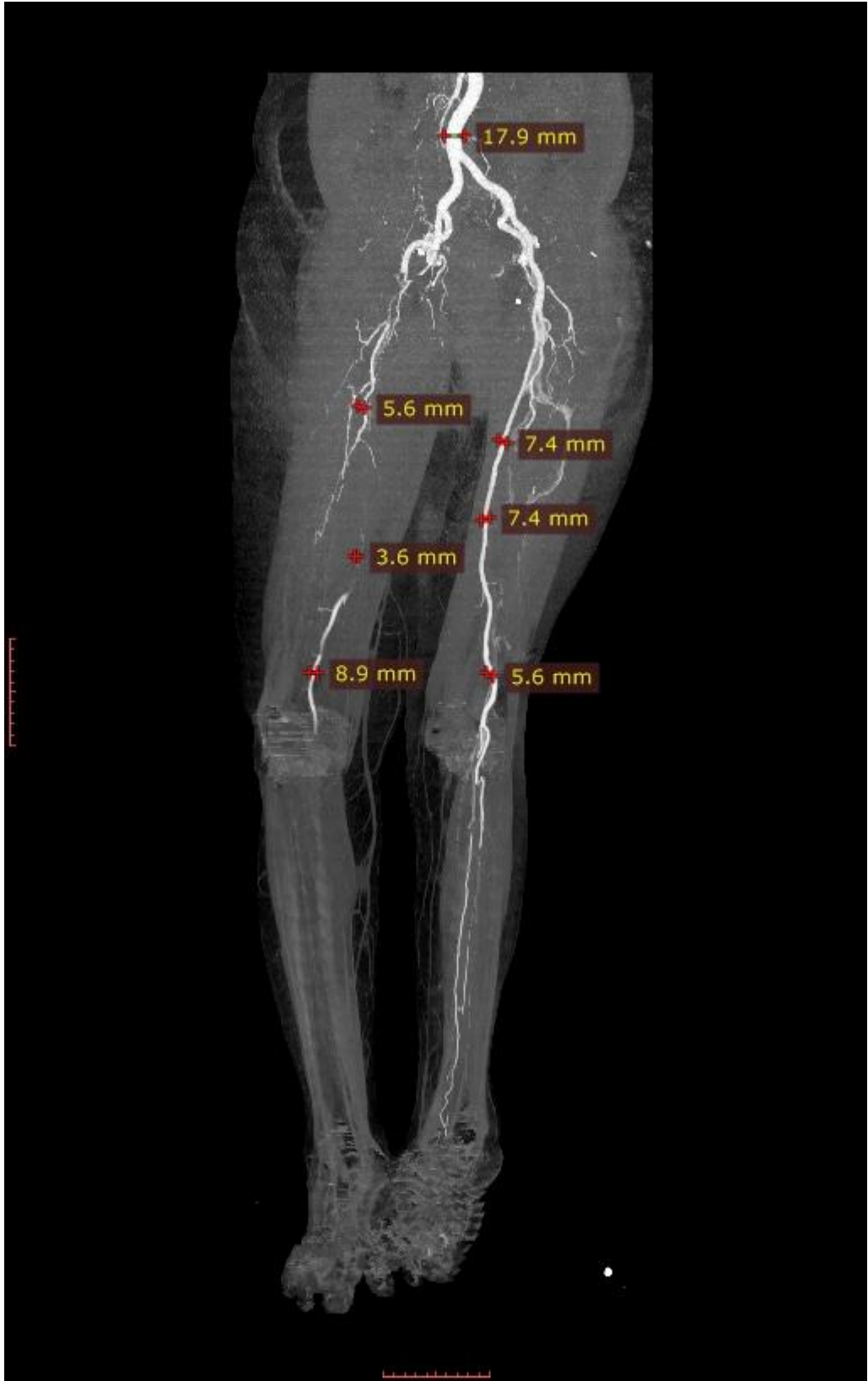
female diabetic



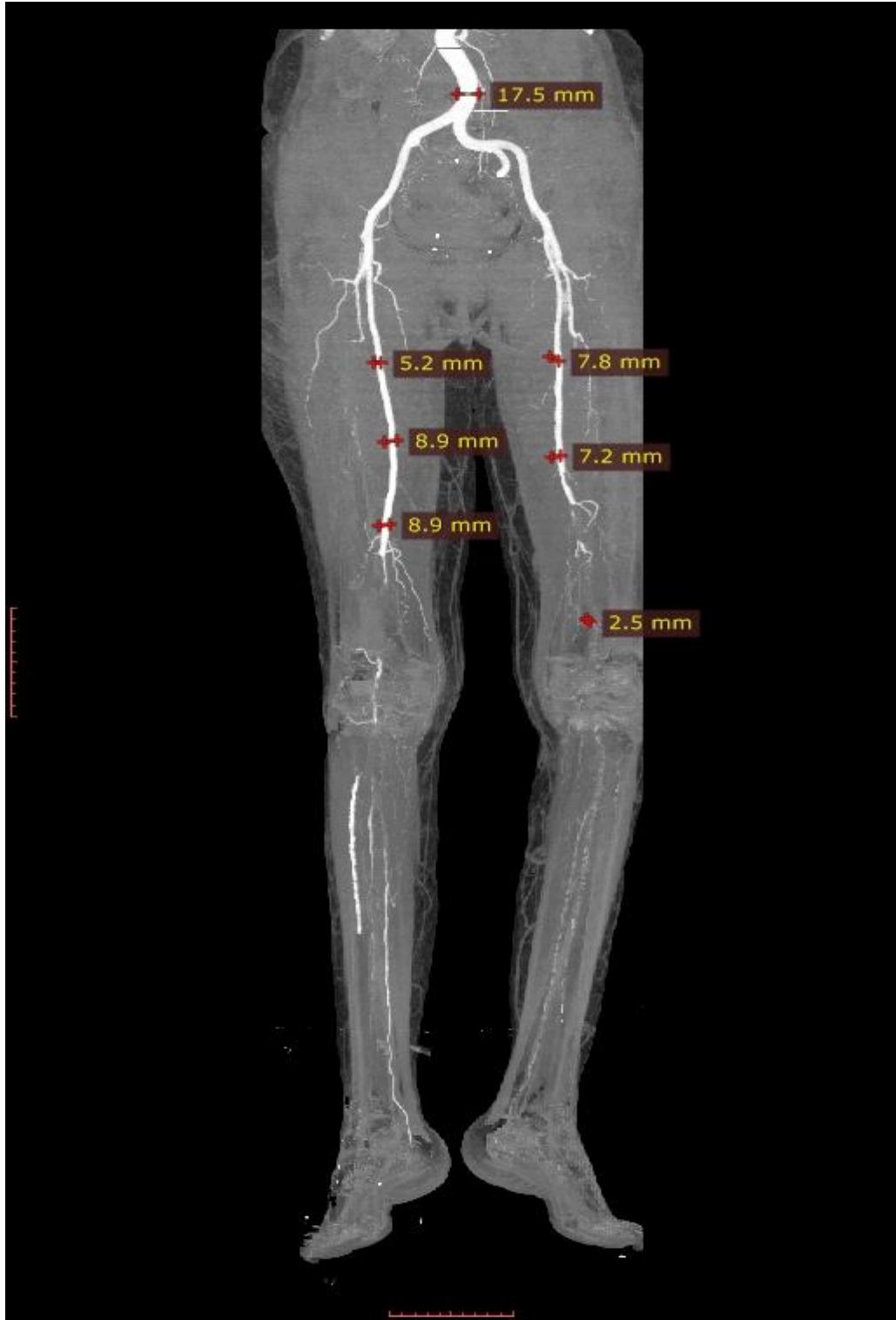
female diabetic



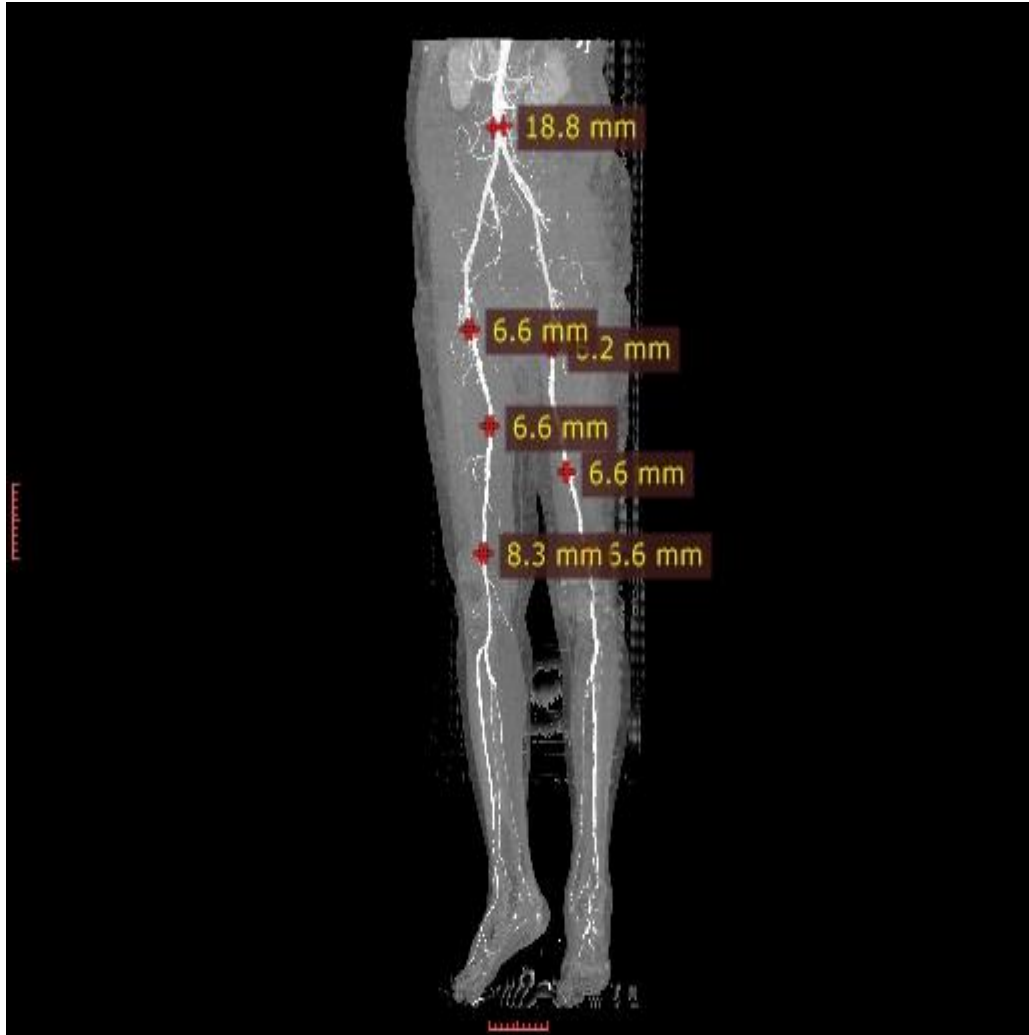
Female hypertensive



Male Hypertensive



Male hypertensive



Male hypertensive